Geochemistry, Geophysics, Geosystems

RESEARCH ARTICLE
10.1029/2019GC008755

High-Resolution Proxy Records From Two Simultaneously Grown Stalagmites From Zoolithencave (Southeastern Germany) and their Potential for Palaeoclimate Reconstruction

Dana F. C. Riechelmann[1], Sylvia Riechelmann[2], Jasper A. Wassenburg[3], Jens Fohlmeister[4,5], Bernd R. Schöne[1], Klaus Peter Jochum[3], Detlev K. Richter[2], and Denis Scholz[1]

[1]Institute for Geosciences, Johannes Gutenberg University Mainz, Mainz, Germany, [2]Institute for Geology, Mineralogy and Geophysics, Ruhr-University Bochum, Bochum, Germany, [3]Max Planck Institute for Chemistry, Climate Geochemistry Department, Mainz, Germany, [4]Potsdam Institute for Climate Impact Research, Potsdam, Germany, [5]Climate Dynamics and Landscape Development, GFZ German Research Centre for Geosciences, Potsdam, Germany

Abstract Two small annually laminated stalagmites from Zoolithencave (southeastern Germany) grew between CE 1821 and 1970 (Zoo-rez-1) and CE 1835 and 1970 (Zoo-rez-2), respectively. Trace element concentrations were determined by Laser Ablation Inductively Coupled Plasma Mass Spectrometry (LA-ICP-MS). Samples for $\delta^{13}C$ and $\delta^{18}O$ analyses were micromilled on annual and subannual resolution. Soil and host rock samples were analyzed by X-Ray Diffraction (XRD) and their elemental concentrations determined via inductively coupled plasma optical emission spectrometer (ICP-OES). Trace element concentrations in the stalagmites show two groups in the principal component analyses: one with Mg, Ba, and Sr and another with Y, P, and Al, respectively. The second group reflects the content of detrital material. Increased weathering of soil minerals seems to have a strong influence on the silicate/carbonate weathering ratio controlling the variability of Mg, Ba, and Sr. Meteorological and Global Network of Isotopes in Precipitation (GNIP) station data were used to calculate the $\delta^{18}O$ values of the drip water (infiltration-weighted, mean annual, and the mean of the winter precipitation $\delta^{18}O$ values) as well as the corresponding speleothem calcite. The $\delta^{18}O$ values calculated by the infiltration-weighted model show similar patterns and amplitudes as the measured $\delta^{18}O$ values of the two stalagmites. This suggests that the $\delta^{18}O$ values of speleothem calcite reflect the $\delta^{18}O$ values of infiltration-weighted annual precipitation, which zis related to mean annual temperature, resulting in a significant correlation between mean annual temperature and the measured $\delta^{18}O$ values of stalagmite Zoo-rez-2. This relationship could potentially be used for quantitative climate reconstruction in the future by extending the time series back in time with further stalagmites from Zoolithencave.

Key Points:
- Silicate versus carbonate weathering has an influence on speleothem trace elements
- Yttrium, phosphorus, and aluminum reflect detrital content of the speleothems
- $\delta^{18}O$ values of the stalagmites are a proxy for mean annual temperature

Supporting Information:
- Supporting Information S1

Correspondence to:
D. F. C. Riechelmann,
riechelm@uni-mainz.de

Citation:
Riechelmann, D. F. C., Riechelmann, S., Wassenburg, J. A., Fohlmeister, J., Schöne, B. R., Jochum, K. P., et al. (2020). High-resolution proxy records from two simultaneously grown stalagmites from Zoolithencave (southeastern Germany) and their potential for palaeoclimate reconstruction. *Geochemistry, Geophysics, Geosystems*, *21*, e2019GC008755. https://doi.org/10.1029/2019GC008755

Received 15 OCT 2019
Accepted 28 APR 2020
Accepted article online 3 MAY 2020

1. Introduction

Quantifying past temperature and precipitation changes is an important but challenging task to set the recent climate change in relation to variations in the past. To achieve this aim, annually to subannually resolved proxy records from climate archives are needed. The most prominent climate archive providing temperature or precipitation reconstructions with annual resolution are tree rings (e.g., Büntgen et al., 2011; Esper et al., 2014; Wilson et al., 2005). Due to the overlap of the tree-ring chronologies with instrumental data, a calibration of the proxy records with meteorological data is possible, and the quantitative reconstruction of climate parameters back in time using the calibration is a standard technique in dendrochronology (Fritts, 1976; Schweingruber, 1983). Speleothems can provide similar high-resolution proxy records, especially if they show annual laminae. A big advantage of speleothems is that they can be precisely dated by the $^{230}Th/U$ method (e.g., Cheng et al., 2013; Richards & Dorale, 2003; Scholz & Hoffmann, 2008), and the derived age-depth models can be further improved by lamina counting, which anchors internal age-models for annual to subannual proxy records (Baker et al., 1993, 2015; Scholz et al., 2012; Smith et al., 2009; Tan et al., 2003; Warken et al., 2018). Speleothem $\delta^{13}C$ and $\delta^{18}O$ values can be measured with annual to subannual resolution and have provided information on past temperature and/or precipitation variability (Boch et al., 2011; Mattey et al., 2008; Myers et al., 2015; Orland et al., 2012; Ridley et al., 2015;

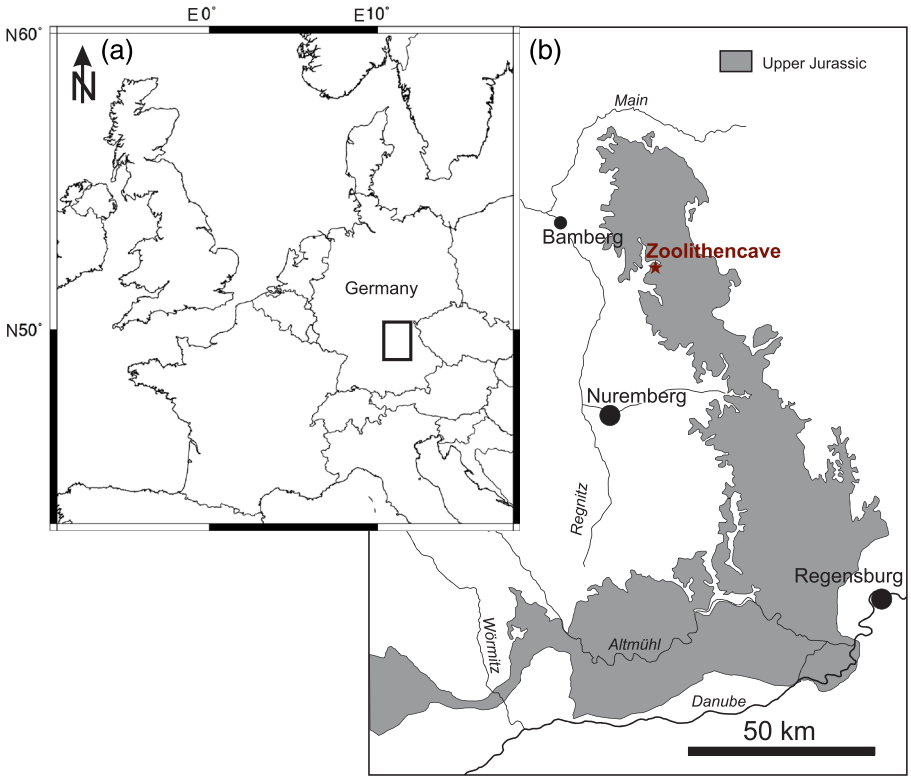

Figure 1. (a) In the map of Central Europe (upper left), the location of map b is indicated by the rectangle. (b) Map of the Franconian Alp indicating the Upper Jurassic containing marl, limestone, and dolomite (modified after Groiß, 1988). The location of the Zoolithencave is indicated by the red star (modified after Riechelmann et al., 2019).

van Rampelbergh et al., 2015). Furthermore, trace elements can be measured at very high spatial resolution. Magnesium, Sr, and Ba have provided information about past precipitation as well as P and Y could be used as proxies for variations in soil and vegetation activity (Borsato et al., 2007; Johnson et al., 2006; Kuczumow et al., 2003; Smith et al., 2009; Treble et al., 2003; Warken et al., 2018). Speleothems containing annual laminae and providing multi proxy records, such as $\delta^{13}C$ and $\delta^{18}O$ values as well as trace element concentrations, that grew until recent times provide the opportunity to calibrate the annual proxies with meteorological data. This allows to quantitatively reconstruct past climate parameters, such as temperature and/or precipitation. For example, Warken et al. (2018) quantified late Holocene autumn/winter precipitation from annual Mg/Ca ratios of a Romanian stalagmite, and Tan et al. (2003) reconstructed summer temperature anomalies for the last 2,650 years from the lamina thickness of a stalagmite from northern China.

In this study, proxy records ($\delta^{13}C$ and $\delta^{18}O$ values and trace element concentrations) from two modern stalagmites from Zoolithencave (southeastern Germany) were tested for their potential to calibrate with meteorological data. This potentially provides the basis for the interpretation of longer Holocene speleothem proxy records from Zoolithencave in the future.

2. Material and Methods

2.1. Cave Setting

Zoolithencave is located in the Franconian Jura in southeastern Germany, 30 km southeast of Bamberg (Figure 1). The host rock of Zoolithencave is Upper Jurassic dolomite (Malm δ, Middle Kimmeridgian), and the cave is famous for its palaeontological inventory (e.g., Esper, 1774; Heller et al., 1972; Rosendahl, 2005). The soil above the cave consists of approximately 15-cm humic A-horizon and approximately 30–40-cm brownish, loamy B-horizon. The average rock overburden of the Entrance Hall is 10–

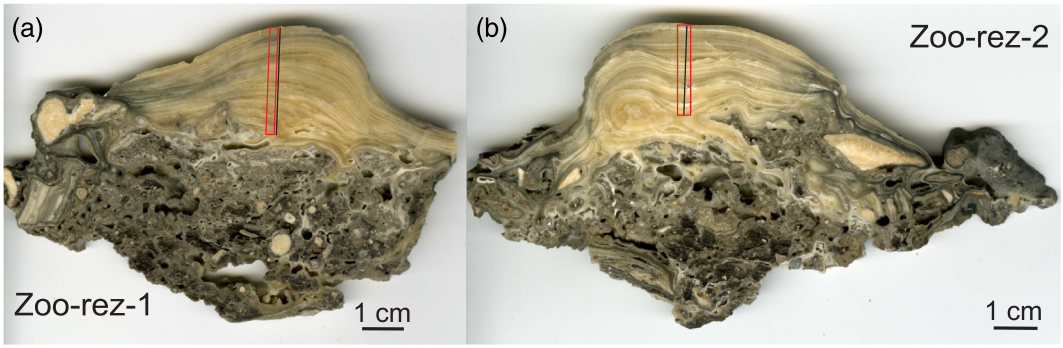

Figure 2. Pictures of the sampled slices of (a) Zoo-rez-1 and (b) Zoo-rez-2. The laser ablation tracks are indicated by black lines, and the milling tracks for the carbon and oxygen isotope samples are indicated by the red rectangles. The sampling tracks in Zoo-rez-1 are a little to the left from the growth axis (5 mm), due to the milling of the ^{14}C samples for the bomb peak detection (see Fig. 2a in Riechelmann et al., 2019). However, Zoo-rez-1 has an asymmetric growth, which gives the impression that the growth axis is located much more to the right. Zoo-rez-1 and -2 were sampled as a block from the cave. The two slices were cut from this block and by visual inspection of the cut slices and the other pieces of the block, we could identify the growth axes of the two stalagmites. The asymmetric growth of Zoo-rez-1 is probably due to the uneven basement.

12 m (Wurth, 2002). The sampling site of the two Zoo-rez stalagmites is approximately 20 m away from the cave entrance (Riechelmann et al., 2019), and first cave air monitoring results show that the temperature in the Entrance Hall is relatively constant at 8.5 ± 0.4°C (Riechelmann et al., 2014) and relative humidity is 94 ± 4% year-round (pers. Comm., Prof. Dr. D. K. Richter, Ruhr-University Bochum). This is comparable to other caves such as Bunker Cave with 10.9 ± 0.6°C and 93 ± 2% relative humidity (Riechelmann et al., 2011). Furthermore, first results from drip water monitoring at a drip site near the sampling site of the two Zoo-rez stalagmites show drip water $\delta^{18}O$ values with a mean of −9.88 ± 0.32‰ (pers. Comm., Prof. Dr. D. K. Richter, Ruhr-University Bochum). This drip site shows a seasonality in the drip rate with mean drip rate of 2.68 ml/min (Riechelmann et al., 2014), and a quick response of the drip rate to main precipitation events within hours is observed (Holz et al., 2018).

2.2. Stalagmites Zoo-rez-1 and -2

Stalagmites Zoo-rez-1 and -2 were sampled as one block in the Entrance Hall of Zoolithencave and grew simultaneously within a distance of 7 cm. Zoo-rez-1 has a height of 3 cm, and Zoo-rez-2 has a height of 2.7 cm (Figure 2). Both stalagmites were sampled in August CE 1999 and described by Wurth (2002). The chronologies were constrained by ^{14}C bomb peak detection at the top of both stalagmites, a ^{14}C age of a piece of charcoal from the consolidated base part of Zoo-rez-2 (Figure 2b), lamina counting, and cross-dating of the lamina thickness series (Riechelmann et al., 2019). Zoo-rez-1 grew between CE 1821 and 1970, whereas Zoo-rez-2 grew from CE 1835 to 1970. The age uncertainty at the top of the two speleothems due to the uncertainty of the ^{14}C bomb peak detection is ±5 years; for the older parts, the uncertainty increases to ±19 years for Zoo-rez-1 and ±7 year for Zoo-rez-2. Both chronologies probably still contain missing and false laminae. However, we were able to minimize the number of missing and false laminae by using the cross-dating of replicated measurements of the same track as well as cross-dating of the three parallel measured tracks on an individual stalagmite. Nevertheless, the missing and false laminae could result in a compression and/or stretching of the chronologies in certain periods. Furthermore, the uncertainty of the ^{14}C bomb peak detection could result in potential differences in the age of the top layers of the two stalagmites (Riechelmann et al., 2019). These uncertainties likely affect correlation coefficients with meteorological data.

2.3. LA-ICP-MS Analyses of Trace Element Concentrations

The element concentrations of the two stalagmites were determined with an Element2 ICP-MS (ThermoScientific, Bremen, Germany) equipped with a high-energy Nd:YAG UP213 laser ablation system (wavelength = 213 nm; New Wave, Fremont, USA) at the Max Planck Institute for Chemistry, Mainz. The reference material used for calibration was NIST SRM 612, a synthetic glass with a high trace

element content (Jochum et al., 2011). The MACS3 (carbonate pressed powder) was measured as a second reference material (Jochum et al., 2012). The measurements were performed in line scan mode near the growth axes of the stalagmites (Figure 2). The spot size of the laser beam was 110 μm, the pulse repetition rate was 10 Hz, and the scan speed was 10 μm/s. The measured isotopes were ^{25}Mg, ^{138}Ba, ^{88}Sr, ^{27}Al, ^{31}P, and ^{89}Y, which were normalized to ^{43}Ca as an internal standard. The 1σ precision of the related NIST SRM 612 measurements was 5.3% for Mg, 3.6% for Ba, 2.3% for Sr, 8.1% for Al, 5.5% for P, and 3.4% for Y. For a detailed description of the methodology, the reader is referred to Jochum et al. (2012) and Mischel et al. (2017).

2.4. Soil and Host Rock Analyses

Four soil samples covering different depths (Zoo B1: 8–23 cm; Zoo B2: 23–34 cm; Zoo B3: 34–41 cm; Zoo B4: 41–43 cm) were collected above Zoolithencave. These samples were analyzed with a Philips Xpert MPD Theta-Theta X-ray Diffractometer (Malvern Panalytical GmbH, Kassel, Germany) using Cu Kα radiation at 45 kV and 40 mA at the Institute for Geology, Mineralogy and Geophysics, Ruhr-University Bochum, to determine the mineralogy of the soil. The scanning range was from 4° to 65° (2θ) with a step size of 0.01° (2θ). The background noise was reduced by using a graphite secondary monochromator.

In order to distinguish between exchangeable and structurally bound ions of clay minerals, a two-step acid-leaching procedure was performed following the method of Wimpenny et al. (2014), which is based on the method of Chan and Hein (2007). For the first leaching step, acetic acid was used, which reflects conditions occurring in natural soils, where carbonic acid is produced by microbial and plant activity. Approximately 200 mg of each dry soil sample was used, and in the first leaching step (exchangeable ions), 5 ml of suprapure acetic acid (4 wt.%) was added, whereas 5 ml of suprapure 2M HCl was used for the second leaching step. Approximately 2 ml of a mixture (1/1) of H_2O_2 (31 wt.%) and HNO_3 (65 wt.%) was added to the dried down leachates to destroy organic matter. Subsequently, the dried down leachates were pestle in a mortar. Additionally, two samples were drilled from the dolomitic host rock.

Both soil and host rock samples were weighed for elemental (Ca, Mg, Sr, and Ba) analyses. The samples were dissolved in HNO_3 (3.5 wt.%) and then diluted with 2-ml MilliQ® H_2O. The elemental concentrations were measured with an inductively coupled plasma optical emission spectrometer (Thermo Fisher Scientific iCAP 6500 DUO, Bremen, Germany) at the Institute for Geology, Mineralogy and Geophysics, Ruhr-University Bochum. The used reference materials were BCS-CRM512 (dolomite; $n = 112$) and BCS-CRM513 (limestone; $n = 110$; Bureau of Analysed Samples Ltd.). The 1σ reproducibility for the two reference materials is 0.19% and 0.32% for Ca, 0.09% and 0.003% for Mg, 21 and 2 μg/g for Sr, and 2 and 22 μg/g for Ba, respectively.

2.5. Carbon and Oxygen Isotope Composition

The samples for stable carbon and oxygen isotope composition of the two stalagmites were obtained with a MicroMill (New Wave Research, Portland, USA) using 300-μm carbide metal drill bit (Dettman & Lohmann, 1995) at the Institute for Geosciences, University of Mainz. The sample resolution is 50 μm for Zoo-rez-1, which approximately results in three samples per year, and 130 μm for Zoo-rez-2, which approximately results in an annual resolution. Sample weights ranged between 60 and 120 μg (± 1 μg). Stable carbon and oxygen isotopes were measured at the Institute for Geosciences at the University of Mainz. Carbonate powder samples were digested in He-flushed borosilicate exetainers at 72°C using 99.999 wt.% phosphoric acid. The released CO_2 gas was then measured in continuous flow mode with a ThermoFisher MAT 253 gas source isotope ratio mass spectrometer coupled to a GasBench II (ThermoScientific, Bremen, Germany). Stable isotope ratios were corrected against an NBS-19 calibrated Carrara marble ($\delta^{13}C = +2.02‰$; $\delta^{18}O = -1.76‰$). Results are expressed as parts per thousand [‰] relative to the Vienna Pee Dee Belemnite [VPDB]. The long-term accuracy based on replicated measurements of the reference materials with known isotopic composition is better that 0.05‰ for both isotope systems.

2.6. Instrumental Meteorological Data

Mean daily temperature [°C], mean daily relative humidity [%] (used for F_{2pm}), daily maximum temperature [°C] (used for T_{2pm}), and daily precipitation sum [mm] were downloaded from the DWD Climate Data Center (www.dwd.de; last access: 12 October 2018) for the meteorological stations Bamberg (CE 1949–

2013; 49.87°N, 10.92°E; 240 m a.s.l.) and Bamberg Observatory (CE 1879–1948; 49.88°N, 10.88°E; 282 m a.s.l.), which are located approximately 30 km north-west of Zoolithencave (Figure 1). Mean annual temperature is 8.5°C, and the mean annual sum of precipitation is 638 mm for the period CE 1879–2013 (Figure S1 in the supporting information). Daily potential evapotranspiration (ET_{pot}) was calculated using the equation of Haude (1954, 1955):

$$ET_{\mathrm{pot}} = h \times P_{2pm} \times \left(1 - \frac{F_{2pm}}{100}\right) \left[\frac{\mathrm{mm}}{\mathrm{day}}\right], \tag{1}$$

with

$$P_{2pm} = 4.54\ \mathrm{hPa} \times 10^{\left(7.45 \times T_{2\mathrm{pm}}/235 + T_{2\mathrm{pm}}\right)}\ [hPa]. \tag{2}$$

$P_{2\mathrm{pm}}$ [hPa] is the saturation vapor pressure, $F_{2\mathrm{pm}}$ [%] is the relative humidity, and $T_{2\mathrm{pm}}$ [°C] is the temperature at 2 pm, respectively. The meteorological station data only provide mean daily relative humidity and not the relative humidity at 2 pm. Therefore, the mean daily relative humidity was used for $F_{2\mathrm{pm}}$. Furthermore, only daily maximum temperatures are provided. Since these should be reached around noon (i.e., near to 2 pm), we used those for $T_{2\mathrm{pm}}$. The composition of vegetation is included in the calculation by the vegetation coefficient h (Häckel, 1999). Vegetation coefficients for beeches were used (Table S1 in the supporting information) as the vegetation above Zoolithencave predominantly consists of this tree species. Dendrochronological analyses of the beeches above the cave in CE 2014 resulted in a maximum tree age of 140 years (pers. Comm., Prof. Dr. A. Bräuning, University Erlangen-Nuremberg). From the daily calculated evapotranspiration, the monthly sum of evapotranspiration was calculated back to CE 1879. The monthly infiltration (*Inf*) was calculated as

$$Inf = Precipitation - ET_{\mathrm{pot}} \quad [\mathrm{mm}]. \tag{3}$$

Negative values for monthly *Inf* [mm], e.g., if ET_{pot} [mm] is larger than the amount of *Precipitation* [mm], were set to zero.

Furthermore, monthly and annual $\delta^{18}O$ values of precipitation were downloaded from the Global Network of Isotopes in Precipitation (GNIP) data base (https://nucleus.iaea.org/Pages/GNIPR.aspx; last access: 12 October 2018) for the GNIP station Regensburg (CE 1978–2013; 49.04°N, 12.10°E; 365 m a.s.l.), which is located approximately 100 km southeast of Zoolithencave (Figure 1). This is the GNIP station with the longest data series (1978–2013) nearby the cave location and has a similar altitude as Zoolithencave (455 m a.s.l.). There is also a GNIP station in Würzburg approximately 100 km northwest of Zoolithencave. The mean annual $\delta^{18}O$ values of precipitation show a positive correlation between both GNIP stations with $r = 0.43$ ($p < 0.01$, $n = 36$, CE 1978–2013). However, comparing the data of the meteorological station Bamberg (mean annual temperature: 9.1°C; mean annual sum of precipitation: 651 mm), the data are more similar with Regensburg (8.8°C; 658 mm) than with Würzburg (9.6°C; 596 mm). Therefore, the GNIP station Regensburg was used.

2.7. Data Analysis

The cross-dated lamina thickness series of both stalagmites provide an assignment of a calendar year to each lamina. However, as described in section 2.2, there is still an age uncertainty for the top lamina of the two stalagmites of ±5 years due to uncertainties in the lag of the ^{14}C bomb peak increase between the atmosphere and the stalagmite as well as uncertainties in the laminae counting procedure, which could not be exactly quantified. This is due to still missing or false laminae, which could result in a compression and/or stretching of the chronologies in different time spans. The cross-dating results in a growth phase of CE 1821 to 1970 for Zoo-rez-1 and of CE 1835 to 1970 for Zoo-rez-2 (Riechelmann et al., 2019). These lamina-based age-depth models for both stalagmites provide the option to assign an age to the different proxy records, which have subannual resolution. This was done using an R Code (R Core Team, 2018) assigning an age to every proxy data point of the trace element, $\delta^{13}C$ and $\delta^{18}O$ time series of both stalagmites using linear interpolation between the counted laminae. For comparison of the proxy data of the two stalagmites and the meteorological data, mean annual values of the trace element, $\delta^{13}C$, and $\delta^{18}O$ time series were

calculated. Proxy records and climate parameters were compared using Pearson correlation coefficients (r) and p values ($p < 0.05$, $p < 0.01$, $p < 0.001$).

All elemental data were standardized prior to principal component analysis (PCA; Navarra & Simoncini, 2010; von Storch & Zwiers, 2002), which was performed using the software PAST3 (Hammer et al., 2001). The PCA was used to identify proxies influenced by the same component.

In order to assess potential parameters affecting the speleothem calcite $\delta^{18}O$ values, the model of Wackerbarth et al. (2010) was applied, which also used the infiltration calculations as presented in section 2.6. The mean annual $\delta^{18}O$ values of the cave drip water were calculated by the Wackerbarth et al. (2010) approach as the sum of the infiltration-weighted monthly mean $\delta^{18}O$ values of meteoric precipitation (GNIP station Regensburg):

$$\delta^{18}O_{\text{drip water}} = \sum_i G_i(T, P, F, h) \times \delta^{18}O_{\text{monthly mean}_i}(T), \tag{4}$$

where *Gi* is the weighting coefficient for each month (Table S2), which depends on temperature, amount of precipitation, relative humidity, and the type of vegetation (see section 2.6 for details). The weighting coefficient is the fraction of the annual amount of water infiltrating into the cave during each month:

$$G_i = \frac{Inf_i}{\sum_i Inf_i}. \tag{5}$$

To calculate the $\delta^{18}O$ values of the stalagmite calcite from the modeled $\delta^{18}O$ values of the drip water, the temperature dependent oxygen isotope fractionation factor from Daëron et al. (2019) was used (equation 7), which is derived from extremely slow-growing cave calcites, precipitated under or very near to equilibrium fractionation conditions. $\delta^{18}O$ values of the drip water are given in [VSMOW], and in the first step, transformed to the [VPDB]-scale (equation 6).

$$\delta^{18}O_{\text{drip water}}\,[VPDB] = \left(\delta^{18}O_{\text{drip water}}[VSMOW] - 30.864\right)/1.030864. \tag{6}$$

Then,

$$\delta^{18}O_{\text{calcite}}\,[VPDB] = \delta^{18}O_{\text{drip water}}[VPDB] + \left(\left(\frac{17570}{T}\right) - 29.13\right), \tag{7}$$

where T is the cave temperature in K (281.65 K). The cave temperature (8.5 ± 0.4°C) corresponds very well to the mean annual temperature above the cave (8.5 ± 0.8°C, CE 1879–2013, meteorological stations Bamberg and Bamberg Observatory). Changes of cave air temperature occur on multiannual to decadal scales (Moore & Sullivan, 1978). Therefore, we assume a constant cave air temperature for the model period. During the time span of CE 1978–2013, the mean annual outside temperature is 9.1°C (meteorological station Bamberg). The current cave air temperature is 8.5°C, corresponding to the mean annual temperature above the cave during CE 1879–2013. This suggests that the increasing outside temperatures are only very slowly transferred to the cave. Unfortunately, the GNIP station from Regensburg only provides $\delta^{18}O$ values of precipitation from CE 1978 to 2013. This time interval does not overlap with the growth interval of the two Zoo-rez stalagmites. Therefore, the modeled time series of $\delta^{18}O$ values of speleothem calcite needs to be extended to the growth phases of the speleothems. The modeled $\delta^{18}O$ values of speleothems calcite are positively correlated with the mean annual temperatures above the cave for CE 1978 to 2013 (Figure 3a). We used this linear regression of the relationship and the instrumental temperature record (CE 1879–1970) to extend the modeled $\delta^{18}O$ values for calcite further back in time:

$$\delta^{18}O_{\text{calcite}} = 0.60 \pm 0.21 \times T - 11.91 \pm 1.90, \tag{8}$$

where T is the mean annual temperature from the meteorological stations Bamberg (CE 1949–1970) and Bamberg Observatory (CE 1879–1948). The 2σ uncertainty of this regression for the modeled $\delta^{18}O$ values of the calcite is ±1.90‰.

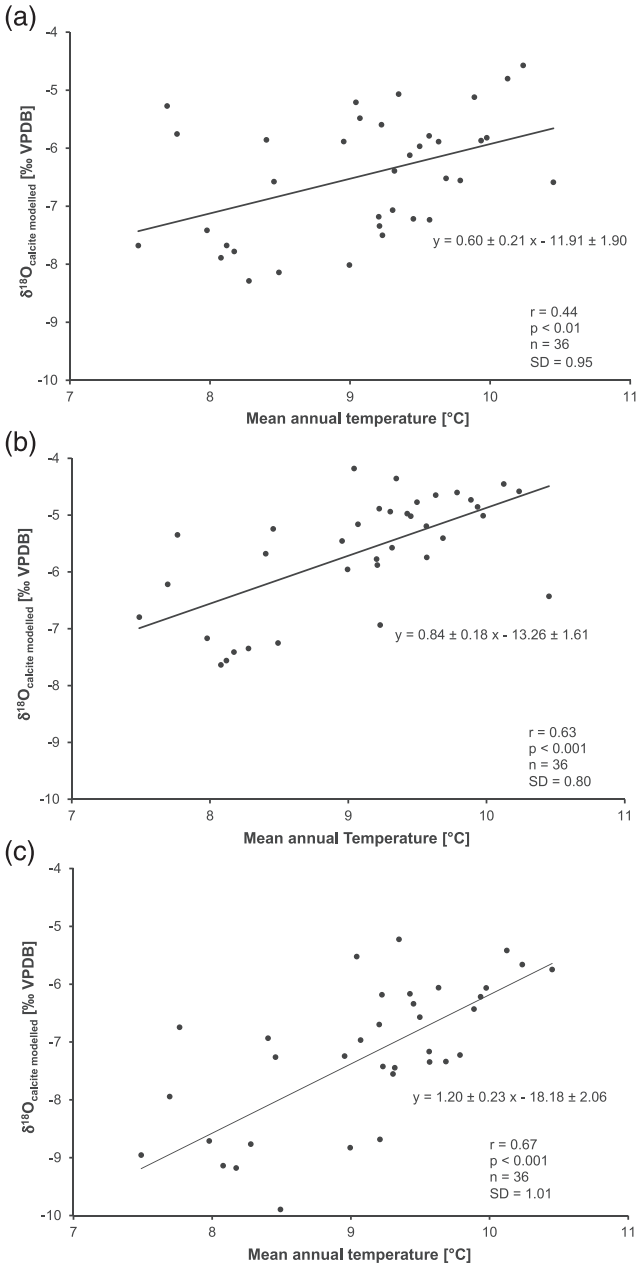

Figure 3. Regression between mean annual temperature of the meteorological station Bamberg (www.dwd.de) and the modeled speleothem calcite $\delta^{18}O$ values according to (a) the model of Wackerbarth et al. (2010) using infiltration-weighted $\delta^{18}O$ values of precipitation, (b) using mean annual $\delta^{18}O$ values of precipitation, and (c) using mean winter $\delta^{18}O$ values of precipitation for the years CE 1978 to 2013. These linear regressions were used to model the $\delta^{18}O$ values for calcite further back in time (CE 1879 to 1970).

However, there is still a debate about which of the different available fractionation factors is best suited for speleothems (Daëron et al., 2019; Hansen et al., 2019; Kim & O'Neil, 1997; Tremaine et al., 2011). Using another fractionation factor than Daëron et al. (2019), only slight changes in the relationship (i.e., within errors) are observed. Furthermore, the fractionation factor only plays a minor role for the calculation of the $\delta^{18}O$ values of the calcite, due to a stronger effect of the temperature dependency of the $\delta^{18}O$ in precipitation in the transfer function.

In addition, we performed a linear regression using the mean annual $\delta^{18}O$ values of the GNIP station, without considering potential evapotranspiration, as equivalent to $\delta^{18}O$ values of the drip water to model $\delta^{18}O$ values of the calcite with equation 7. We are aware that it is unlikely that the complete annual amount of precipitation reaches the cave as drip water. However, this gives us an idea about the potential maximum extreme values because all precipitations from the summer half-year with higher $\delta^{18}O$ values are included in this model. This results in a linear relationship between mean annual temperature (CE 1978–2013) and the modeled $\delta^{18}O$ values of the calcite (Figure 3b) of:

$$\delta^{18}O_{\text{calcite}} = 0.84 \pm 0.18 \times T - 13.26 \pm 1.61. \quad (9)$$

The 2σ uncertainty of this regression for the modeled $\delta^{18}O$ values of the calcite is ±1.60‰.

Finally, a third linear regression was performed using the mean winter $\delta^{18}O$ values of the GNIP station to model the $\delta^{18}O$ values of the calcite with equation 7. For the mean winter $\delta^{18}O$ values, the months January to March and October to December were used because these are the months in the long-term data, where most of the precipitation infiltrated (Figure S1 and Table S2). Therefore, this assumption gives us an idea about the potential minimum extreme values because only precipitation from the winter half-year with lower $\delta^{18}O$ values is considered in this model. This third linear relation (Figure 3c) is described by the following equation:

$$\delta^{18}O_{\text{calcite}} = 1.20 \pm 0.23 \times T - 18.18 \pm 2.06, \quad (10)$$

and the 2σ uncertainty of this regression for the modeled $\delta^{18}O$ values of the calcite is ±2.02‰. The different equations for these three scenarios were used to model the $\delta^{18}O$ values of the calcite between CE 1879 and 1970 from the temperature record of the Bamberg meteorological stations to compare the modeled $\delta^{18}O$ series with the measured $\delta^{18}O$ series of the two stalagmites.

3. Results

3.1. Element Concentrations

The Mg series of Zoo-rez-1 and -2 shows pronounced cycles (Figure 4a). However, counting the minima of both series results in 123 minima for Zoo-rez-1 and 93 minima for Zoo-rez-2, which does not correspond to the length of the two time series (150 and 133 years, respectively). Barium and Sr cycles correlate positively with Mg as shown by the results of the PCA (Figure 5), albeit their amplitudes are smaller (Figures 4b and 4c).

The second group of trace elements in the PCA is formed by Y, P, and Al (Figure 5), which show elevated values at the same time in all three elemental records (Figures 4d–4f). In the PCA of Zoo-rez-2

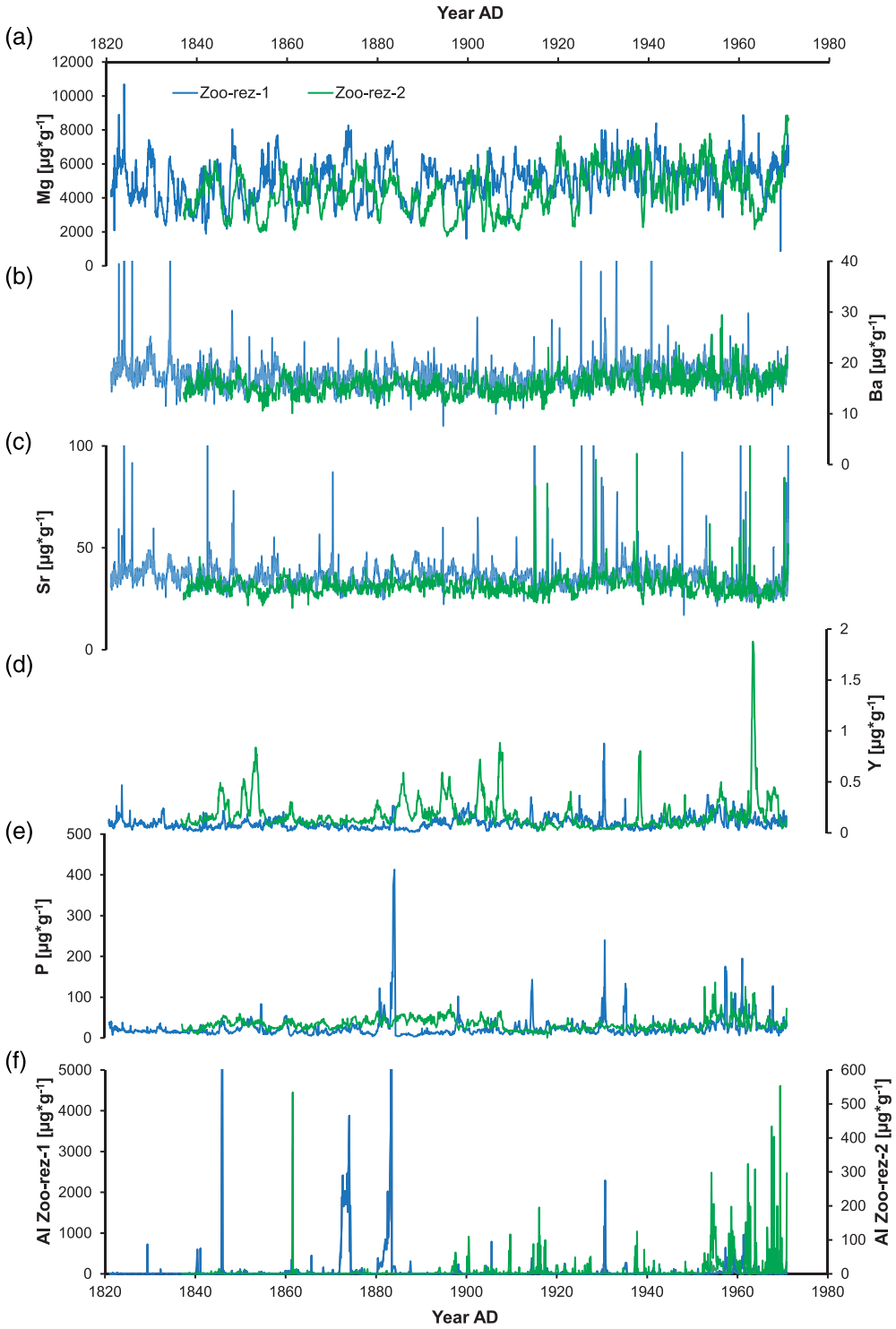

Figure 4. Trace element proxy records are shown against year CE for (a) Mg, (b) Ba, (c) Sr, (d) Y, (e) P, and (f) Al for the two stalagmites Zoo-rez-1 and -2.

(Figure 5b), Y shows an anticorrelation with Mg, Sr, and Ba. The two stalagmites show similar mean values for all elements (Figures 4a–4e) except for Al, where Zoo-rez-1 has a much higher concentration than Zoo-rez-2 (mean value: 71 compared to 12 µg/g, Figure 4f).

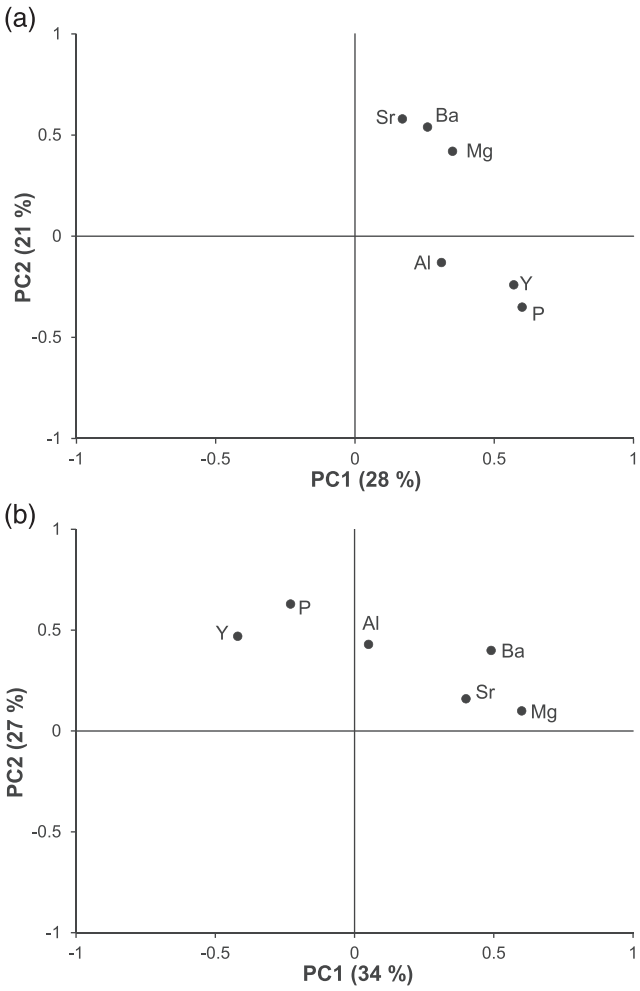

Figure 5. Principal component analyses (PCA) for the six different elements of the two stalagmites (a) Zoo-rez-1 and (b) Zoo-rez-2.

3.2. Soil Mineralogy and Elemental Concentrations

The soil above Zoolithencave consists of quartz, feldspar (plagioclase, orthoclase), kaolinite, illite/muscovite, and chlorite (XRD analysis, Figure S2). There are no differences in the mineralogical composition of the soil samples through the soil-depth profile. Calcium, Mg, and Sr concentrations of the soil samples are generally higher for samples treated with acetic acid compared to those treated with HCl (Table 1). Samples from greater depths (34–43 cm) display significantly higher Ca, Mg, and Sr concentrations (Zoo B3 and B4). For Ba, we observed no significant difference between acetic acid and HCl leachates, and the concentrations vary between 148 and 376 μg/g (Table 1). The dolomitic host rock displays high Ca and Mg concentrations, whereas Sr and especially Ba concentrations are very low (Table 1).

3.3. $\delta^{13}C$ and $\delta^{18}O$ Values

The mean $\delta^{18}O$ values of the two stalagmites are similar, i.e., -6.70 ± 0.50‰ for Zoo-rez-1 and -7.04 ± 0.48‰ for Zoo-rez-2. In some sections (around CE 1870 and 1920), the pattern of the two stalagmites are quite similar, whereas in other sections, differences are visible (e.g., CE 1940 to 1970, Figure 6a). Two pronounced negative peaks are in amplitude and absolute values very similar: one around CE 1875 and the other one around CE 1920. However, the $\delta^{18}O$ values of Zoo-rez-1 are generally slightly higher (0.34‰) compared to the $\delta^{18}O$ values of Zoo-rez-2. Both stalagmites show a positive long-term trend in the $\delta^{18}O$ values. The mean $\delta^{13}C$ values of the two stalagmites show a larger difference than the mean $\delta^{18}O$ values with -8.62 ± 0.56‰ for Zoo-rez-1 and -9.20 ± 0.85‰ for Zoo-rez-2. Furthermore, a common pattern, as observed for the $\delta^{18}O$ records, is not visible (Figure 6b). For example, around CE 1900, the two stalagmites show a discrepancy of up to 3‰.

The correlation coefficients between the $\delta^{13}C$ and $\delta^{18}O$ records are 0.46 ($p < 0.001$, $n = 500$) for Zoo-rez-1 and 0.66 ($p < 0.001$, $n = 142$) for Zoo-rez-2 (Figure S3). Calculating the $\delta^{18}O$ value for the calcite, precipitating from recent mean $\delta^{18}O$ values of the drip water (-9.88 ± 0.32‰ [VSMOW]) using the fractionation factor of Daëron et al. (2019) (equation 7), results in -6.27‰ [VPDB], which is in agreement with the $\delta^{18}O$ values measured in the two stalagmites within uncertainties.

3.4. Annual Proxy Data

For comparison of all proxy records, mean annual values were calculated for the element concentrations as well as the $\delta^{13}C$ and $\delta^{18}O$ values. The annual lamina thickness series of both stalagmites does not show any highly significant correlations ($p < 0.001$) with the proxy records (Table 2). The $\delta^{13}C$ and $\delta^{18}O$ series show a positive correlation of 0.50 ($p < 0.001$, $n = 150$) for Zoo-rez-1 and 0.69 ($p < 0.001$, $n = 113$) for Zoo-rez-2, respectively, which are slightly higher than the correlation coefficients obtained for the measured high-resolution data. Furthermore, the $\delta^{18}O$ values covary positively with the Mg content ($p < 0.001$) in both stalagmites and show a negative correlation ($p < 0.001$) with P in Zoo-rez-2. The $\delta^{13}C$ values show a positive correlation ($p < 0.001$) with Y in Zoo-rez-1 and a positive correlation ($p < 0.001$) with Ba, Mg, and Y in Zoo-rez-2. For the element concentrations, the same pattern is visible for the annually resolved data and the high-resolution data. Mg, Ba, and Sr as well as Y and P are positively correlated ($p < 0.001$). Yttrium shows a negative correlation ($p < 0.001$) with Mg and Sr in Zoo-rez-2. Aluminum shows a positive correlation ($p < 0.001$) with Mg and P in Zoo-rez-1 and with Ba and Sr in Zoo-rez-2 (Table 2).

Table 1
Element Concentrations (Ca, Mg, Sr, and Ba) and Element to Ca Ratios of Dolomitic Host Rock, Soil Samples Leached with Acetic Acid and HCl as well as Mean Values for the Two Stalagmites

Sample name	Ca (µg/g)	Ca (mmol/L)	Mg (µg/g)	Mg (mmol/L)	Mg/Ca	Sr (µg/g)	Sr (mmol/L)	Sr/Ca	Ba (µg/g)	Ba (mmol/L)	Ba/Ca
Host rock	235,770	5,883	112,400	4,625	0.786	63	0.72	0.0001	2	0.015	0.000002
Host rock	238,400	5,948	121,000	4,978	0.837	60	0.68	0.0001	1	0.007	0.000001
Zoo B1 acetic acid	8,262	206	3,380	139	0.675	15	0.17	0.0008	245	1.784	0.009
Zoo B2 acetic acid	4,552	114	2,735	113	0.991	4	0.05	0.0004	376	2.738	0.024
Zoo B3 acetic acid	72,759	1,815	36,280	1,493	0.822	30	0.34	0.0002	273	1.988	0.001
Zoo B4 acetic acid	70,192	1,751	38,040	1,565	0.894	23	0.26	0.0001	168	1.223	0.001
Zoo B1 HCl	1,512	38	6,765	278	7.378	6	0.07	0.0018	148	1.078	0.029
Zoo B2 HCl	2,919	73	10,220	420	5.773	10	0.11	0.0016	293	2.134	0.029
Zoo B3 HCl	12,830	320	12,590	518	1.618	13	0.15	0.0005	279	2.032	0.006
Zoo B4 HCl	9,435	235	12,790	526	2.235	9	0.10	0.0004	291	2.119	0.009
Zoo-rez-1	—	—	5,045	208	0.022	36	0.41	0.00004	18	0.131	0.00001
Zoo-rez-2	—	—	4,370	180	0.019	31	0.35	0.00004	16	0.117	0.00001
Mean values											
Host rock	237,085	5,916	116,700	4,801	0.812	62	0.70	0.0001	1,5	0.011	0.000002
Soil	22,808	569	15,350	632	2.548	14	0.16	0.0007	259	1.887	0.013
Speleothem			4,708	194	0.020	34	0.38	0.00004	17	0.124	0.00001

4. Discussion

4.1. Trace Elemental Variations of Soil and Host Rock

Leaching the soil by acetic acid, as used in the first step, reflects conditions occurring in natural soils, where carbonic acid is produced by microbial and plant activity. In this first acid-leaching step, mostly exchangeable ions of clay minerals, such as Mg, Sr, and Ca, are detached. Thus, the higher concentrations of these elements for the deeper soil samples leached by acetic acid are probably due to a higher abundance of clay minerals in the deeper parts of the soil. By using HCl, structurally bound ions are leached from the minerals. In this case, Mg is derived from chlorite and possibly also from illite (Okrusch & Matthes, 2005; Wimpenny et al., 2014), which are more abundant in deeper soil sections explaining the higher concentrations for the two deepest samples (Table 1). The mineral feldspar, however, can already be weathered under the presence of carbonic acid and subsequently forms kaolinite (Okrusch & Matthes, 2005). Thus, the high Ca concentrations for both the acetic acid and HCl leachates can be explained by the weathering of Ca-bearing plagioclase. Consequently, Ca and Mg are derived from (i) easily leachable sites (ion exchangeable) and (ii) structural sites. This is also the case for Sr, although no mineral containing Sr in its crystal lattice was observed by XRD. However, Sr most likely substitutes for other cations in the crystal lattice. The relatively constant concentrations of Ba for both acid-leaching steps are best explained by the presence of feldspar containing Ba. Mixed crystals between orthoclase ($KAlSi_3O_8$) and celsian ($BaAl_2Si_2O_8$), the hyalophane, provide Ba due to the high weathering sensitivity of feldspar (Okrusch & Matthes, 2005). The Mg concentration of the host rock is high due to its dolomitic composition; however, Sr concentrations are much lower, and even Ba shows a very low concentration in the dolomite.

4.2. Trace Element Variations of Speleothems

Phosphorus and Y show a positive correlation in both stalagmites and form one group in the PCA (Table 2, Figure 5). Both elements are mostly transported into the cave associated with colloids, such as humic and other organic substances from the soil (Fairchild & Treble, 2009), and subsequently incorporated into the stalagmite calcite. The high organic content of both stalagmites is visible in the UV-fluorescence, which is induced by humic and fulvic acids (Baker et al., 1993; Riechelmann et al., 2019; Shopov, 2003). Phosphorus originates most likely from microbial breakdown of organic matter in the soil, and Y is adsorbed to organic matter, which results in a positive correlation of P and Y (Borsato et al., 2007). Therefore, P and Y have been interpreted as proxies for vegetation productivity and microbial activity in the soil in several speleothem trace element studies (Borsato et al., 2007; Fairchild & Treble, 2009; Treble et al., 2003; Wassenburg et al., 2012). Decreasing P and Y concentrations are related to decreasing microbial breakdown of organic matter and lower vegetation productivity, which are affected by decreasing temperatures or precipitation

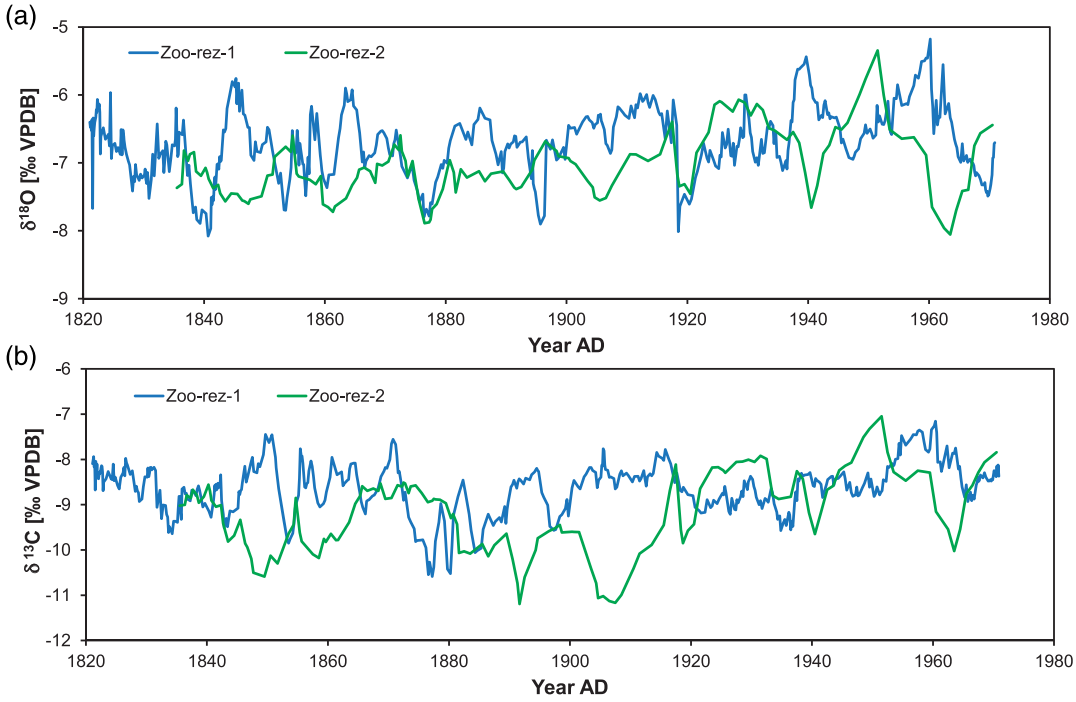

Figure 6. (a) $\delta^{18}O$ records and (b) $\delta^{13}C$ records shown against year CE of the stalagmites Zoo-rez-1 and -2.

and vice versa (Borsato et al., 2007; Treble et al., 2003; Wassenburg et al., 2012). In many cases, both elements peak after an increase of infiltration in autumn indicating more effective transport of organic colloids from the soil into the cave during this season ("autumnal flush") (Borsato et al., 2007; Frisia et al., 2012; Huang et al., 2001; Treble et al., 2003). Unfortunately, P and Y cannot be used as proxies for vegetation and soil activity in the Zoo-rez stalagmites because the signal is also influenced by detrital contamination related to silicates. Aluminum is a proxy for detrital material in speleothems because it is transported to the cave

Table 2
Correlation Coefficients for All Proxies on Annual Resolution

Zoo-rez-1	Al	Ba	Mg	Sr	P	Y	$\delta^{13}C$	$\delta^{18}O$
Ba	0.08							
Mg	**0.28**	**0.45**						
Sr	−0.02	**0.43**	**0.21**					
P	**0.54**	0.09	0.22	−0.04				
Y	0.01	0.09	0.09	0.00	**0.44**			
$\delta^{13}C$	−0.14	0.02	*0.17*	−0.12	0.07	**0.33**		
$\delta^{18}O$	0.00	*0.16*	**0.27**	0.00	*0.16*	0.22	**0.50**	
Lamina thickness	−0.11	0.15	0.10	0.12	−0.07	−0.03	0.14	−0.03
Zoo-rez-2								
Ba	**0.31**							
Mg	0.14	**0.79**						
Sr	**0.30**	**0.57**	**0.58**					
P	−0.06	0.12	−0.18	−0.12				
Y	0.13	−0.14	**−0.50**	**−0.32**	**0.59**			
$\delta^{13}C$	0.17	**0.40**	**0.51**	*0.22*	−0.29	**0.38**		
$\delta^{18}O$	0.01	*0.18*	**0.32**	0.24	**−0.31**	−0.29	**0.69**	
Lamina thickness	0.29	−0.07	−0.12	−0.14	−0.03	0.04	−0.08	*−0.19*

Note. Numbers in italics show p values < 0.05; numbers underlined show p values < 0.01; numbers in bold show p values < 0.001 (n = 150 for Zoo-rez-1 and n = 113–136 for Zoo-rez-2).

as particles, such as clay minerals, which are rich in Al (Fairchild & Treble, 2009; Wassenburg et al., 2012). In particular, Al shows a positive correlation with P in Zoo-rez-1 (Table 2) and forms one group with P and Y in the PCA for both stalagmites (Figure 5). Several peaks in Al of Zoo-rez-1 are also visible in P and Y of Zoo-rez-1 (Figures 4d–4f). Although, Zoo-rez-2 contains less Al (mean value 12 μg/g), higher Al values in the top section of the stalagmite are also associated with increased P and Y in the top part of Zoo-rez-2 (Figures 5d–5f). Thus, detrital contribution to P and Y is very likely.

A positive correlation between speleothem Mg, Ba, and Sr (Figure 5, Table 2) is most commonly interpreted as an indicator of prior calcite precipitation (PCP) (Fairchild et al., 2000, 2006; Johnson et al., 2006; Smith et al., 2009; Tooth & Fairchild, 2003; Treble et al., 2003). PCP describes the precipitation of calcite prior to precipitation of carbonate on the top of the stalagmite, which might occur in air filled pockets and cavities in the aquifer above the cave and/or at the cave ceiling as stalactites or other sinter forms. PCP increases the Mg, Sr, and Ba to Ca ratios of the drip water and, hence, in speleothem calcite (Fairchild et al., 2006). Enhanced PCP is most pronounced in the summer season, when infiltration is at a minimum, or under drier climate conditions associated with longer drip intervals (Fairchild et al., 2006; Fairchild & Treble, 2009; Treble et al., 2003; Wassenburg et al., 2012, 2020). A simple test to assess whether PCP is a major controlling factor for variations in the elemental concentrations is plotting ln (Mg/Ca) versus ln (Sr/Ca) and calculating the slope of the regression line (Sinclair et al., 2012). Wassenburg et al. (2020) modeled different PCP slopes compared to Sinclair et al. (2012) and showed that PCP may be associated with slopes between 0.71 and 1.45 depending on whether the Sr partitioning coefficient is related to the Mg/Ca ratio of the speleothem calcite. The slopes calculated for Zoo-rez-1 and -2 are 0.20 and 0.18, respectively (Figure 7). Therefore, we conclude that the Mg, Ba, and Sr variations in Zoo-rez-1 and -2 are most likely not dominated by PCP and have to be influenced by other factors.

Growth rate could be an influencing factor of the Sr and Ba variations due to their growth rate dependent partitioning coefficients (Borsato et al., 2007; Treble et al., 2005; Warken et al., 2018). However, since the partitioning coefficient of Mg is not growth rate dependent, the positive correlation between Mg, Sr, and Ba can probably not be explained by variations in growth rate. Furthermore, a correlation between the lamina thickness series, which reflects the annual growth rate, and Ba or Sr is not observed in the two stalagmites (Table 2). Therefore, growth rate can be excluded as an influencing factor.

The sources of Ca, Mg, and Sr in the speleothems from Zoolithencave are the soil and host rock (especially for Ca and Mg), whereas Ba mostly results from the soil as discussed in section 3.4 (Table 1). Nevertheless, the Mg of the stalagmites probably originates in large parts from the dolomitic host rock (Table 1) because the amount of Ca originating from the host rock is higher than from the soil. The Sr of the stalagmites originates both from the dolomite and the soil. The exchangeable ions also display an increase of Sr with soil depth, which is not the case for Ba. For comparison to this case, that Ba could be mainly provided from the soil, was also detected in drip water from a cave in southeast Australia, where the host rock did not contain any Ba (Rutlidge et al., 2014). Therefore, the changing amount of leaching from the soil is an important factor causing a positive correlation between Mg, Sr, and Ba. Longer water residence time in the soil, induced by drier climate conditions as well as higher temperatures, increases silicate weathering, which results in changes in the silicate (feldspar and clay minerals) versus carbonate (dolomite) weathering ratio. However, carbonate weathering is always dominant and can thus be considered as more or less constant in the temperate climate zone (Egli et al., 2008; Maher, 2010; Tipper et al., 2006). Therefore, changes in silicate weathering are most likely responsible for variations in the silicate/carbonate weathering ratio. There is a significant negative correlation between temperature and infiltration for the months May to September (CE 1879–2013) (Figure S1 and Table S2). Warmer and drier summers probably increase the silicate/carbonate weathering ratio, and more Mg, Sr, and Ba are derived from the soil than during colder and wetter climate conditions.

Dry conditions also favor PCP, which enhances the Mg, Sr, and Ba concentrations in the same direction. Significant positive correlations ($p < 0.001$) of Mg and Ba with the $\delta^{13}C$ values of stalagmite Zoo-rez-2 indicate that PCP has a minor influence (Fairchild & Treble, 2009; Johnson et al., 2006), due to not very high correlation coefficients (Table 2). For Zoo-rez-1, the correlation between Mg and $\delta^{13}C$ is weak ($p < 0.05$), which suggests that the Mg content of this stalagmite is also influenced by another factor. This is probably detrital material as suggested by the weak but significant correlation ($p < 0.01$) between Al and Mg (Table 2). Due to

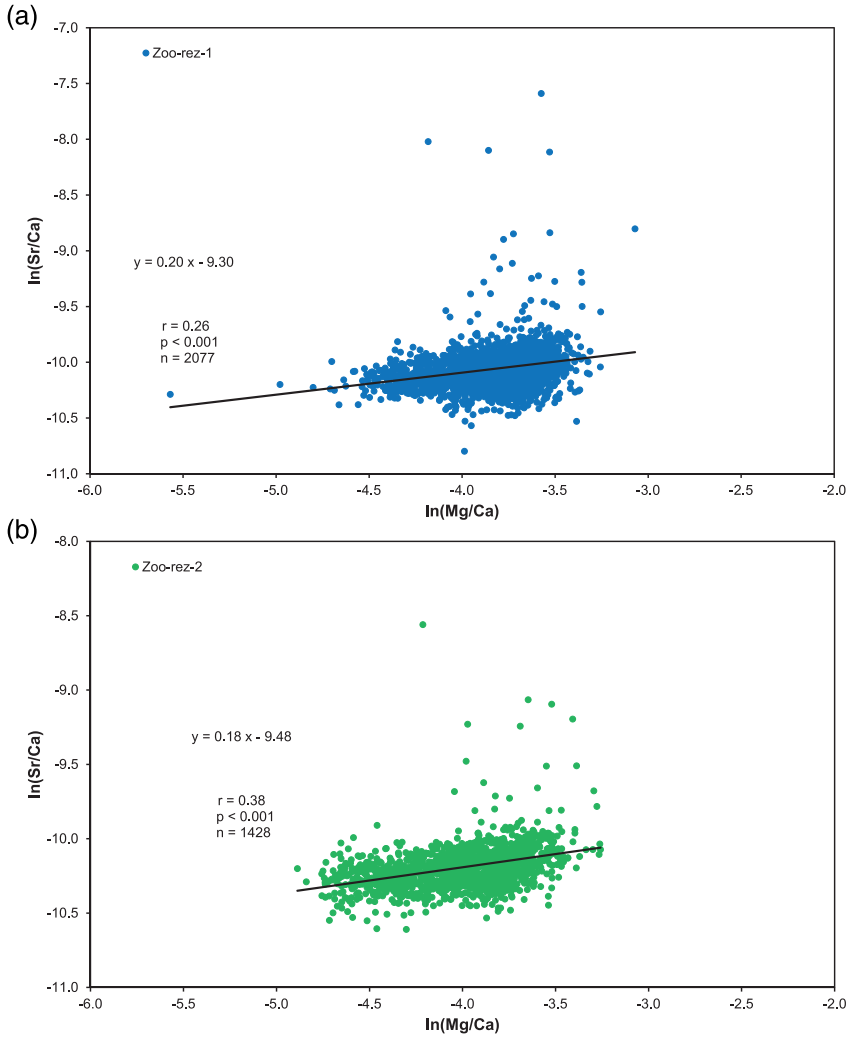

Figure 7. ln (Mg/Ca) plotted against ln (Sr/Ca) for (a) Zoo-rez-1 and (b) Zoo-rez-2 to test for prior calcite precipitation (PCP) after Sinclair et al. (2012).

the smaller partitioning coefficient for Mg in comparison to Sr and Ba, PCP would be most pronounced for Mg. However, it is likely that the lower slopes of the trend lines in Figure 7 are related to changes in the initial concentrations of these elements, which are related to changes in the silicate/carbonate weathering ratio. The two processes, changes in the silicate/carbonate weathering ratio and PCP, cannot be disentangled.

A positive correlation is also observed between $\delta^{18}O$ values and Mg content for both stalagmites (Table 2). However, these correlations are weak, which shows that PCP and drip rate seem to have a minor effect on these proxies (Deininger et al., 2012; Johnson et al., 2006; Mühlinghaus et al., 2009; Riechelmann et al., 2013). A more likely explanation for the positive correlation between the Mg content and $\delta^{18}O$ values involves a relation to temperature because $\delta^{18}O$ values are influenced by mean annual temperature (section 4.3.4) and Mg is related to increased silicate/carbonate weathering ratio during warmer and drier summers, which is recorded at annual resolution in the stalagmite.

Zoo-rez-2 shows significant negative correlations between Mg and Y and Sr and Y, which are not visible for Zoo-rez-1 due to Y and P being strongly affected by detrital material. This negative correlation of Mg and Sr with Y may be explained by warmer and drier conditions inducing an increased silicate/carbonate weathering ratio and also result in a reduction of soil activity (Borsato et al., 2007; Treble et al., 2003; Wassenburg et al., 2012). This would in turn result in lower Y concentrations and explain the negative correlation between Mg and Y (Table 2).

4.3. $\delta^{13}C$ and $\delta^{18}O$ Values

4.3.1. Equilibrium Versus Disequilibrium Fractionation During Calcite Precipitation

The significant positive correlation between the $\delta^{13}C$ and $\delta^{18}O$ values observed for both stalagmites (Table 2, Figure S3) indicates disequilibrium fractionation during calcite precipitation as suggested by several other studies (Boch & Spötl, 2011; Fohlmeister et al., 2017; Hendy, 1971; Mattey et al., 2008; Mickler et al., 2004; Mühlinghaus et al., 2009; Riechelmann et al., 2013). The correlation between the $\delta^{13}C$ and $\delta^{18}O$ values is higher for Zoo-rez-2 than for Zoo-rez-1, which could indicate stronger disequilibrium fractionation during calcite precipitation for Zoo-rez-2. On the other hand, Zoo-rez-2 shows lower $\delta^{13}C$ and $\delta^{18}O$ values than Zoo-rez-1, which suggests stronger disequilibrium fractionation during calcite precipitation for Zoo-rez-1 or more and constant PCP. Calculating the $\delta^{18}O$ value for calcite precipitated in equilibrium, using the equation of Daëron et al. (2019) (equation 7), and the mean $\delta^{18}O$ value of drip water collected in the framework of the preliminary monitoring program (-9.88 ± 0.32‰, [CE 2011–2013]; pers. Comm., Prof. Dr. D. K. Richter, Ruhr-University Bochum) and the cave temperature of 8.5°C (Riechelmann et al., 2014), gives -6.27 ± 0.31‰. Calculating the potential $\delta^{18}O$ values of drip water for these three years from the infiltration-weighted $\delta^{18}O$ values of the precipitation of the GNIP station results in a value of -9.89 ± 0.70‰. This is in agreement with the measured $\delta^{18}O$ values of the drip water and also indicates the reliability of the infiltration-weighted model (section 4.3.4). The calculated $\delta^{18}O$ values for the calcite precipitating in equilibrium from this solution (−6.27‰) is higher than the most recent (CE 1970) $\delta^{18}O$ values of Zoo-rez-1 (−7.05‰) and Zoo-rez-2 (−6.44‰), as well as the mean $\delta^{18}O$ values of Zoo-rez-1 (−6.70‰) and Zoo-rez-2 (−7.04‰). The higher calculated $\delta^{18}O$ value for the calcite could be caused by higher $\delta^{18}O$ values in precipitation due to higher mean annual temperatures in the recent time. Therefore, lower $\delta^{18}O$ values of the stalagmites in the past are most probable related to the decreasing mean annual temperature back in time (Figure 8). This may indicate that the stalagmites grew relatively close to $\delta^{18}O$ equilibrium conditions. However, disequilibrium conditions and also a variable degree in the amount of disequilibrium during the growth of the stalagmites cannot be excluded.

4.3.2. Signal Transfer Time, Ventilation, and Evaporation

The maximum amplitudes of both stalagmites are up to 4‰ for $\delta^{13}C$ and up to 2.5‰ for $\delta^{18}O$ values. The high amplitude of the $\delta^{18}O$ values could be explained by the corresponding amplitude of 3.7‰ in the mean annual $\delta^{18}O$ values of precipitation, although GNIP station data and the stalagmite growth do not overlap. The signal is transferred relatively fast due to the low rock overburden. This short transfer time is also the reason for the observed annual lamination in the stalagmites (Riechelmann et al., 2019). For speleothem $\delta^{13}C$ values, the amplitudes are generally higher than for $\delta^{18}O$ values (Mühlinghaus et al., 2009; Scholz et al., 2009), which agrees with the observation for Zoo-rez-1 and -2. Long-term changes in the ventilation of the cave do probably not play a role during the growth of Zoo-rez-1 and -2, because the cave entrance was closed by a door sometime after the 1970s and was constantly open before (pers. Comm. M. Conrad). In addition, no other changes of the cave environment are documented to have happened earlier. However, both stalagmites show lower $\delta^{18}O$ values than the $\delta^{18}O$ value calculated for equilibrium conditions for the most recent time. This indicates that evaporation or ventilation do not play an important role during the growth of both stalagmites.

4.3.3. Vegetation

A change in vegetation is a possibility to change the $\delta^{13}C$ values. The oldest trees above the cave are approximately 140 years old (growth started in CE 1874, pers. Comm., Prof. Dr. A. Bräuning, University Erlangen-Nuremberg), while the speleothems are 150 and 136 years old (started growth in CE 1821 and 1835), respectively. It is possible that the density of the forest increased over time. Historical documents indicate a vegetation consisting of juniper heath used for sheep grazing above the cave around CE 1800 and a change to forest around CE 1900 (Lang, 2000). Nowadays, there is a relatively dense beech forest above the cave, which most probably developed during the growth period of the stalagmites. However, we do not see a long-term trend in the $\delta^{13}C$ values. Therefore, a correlation of these vegetation changes and the $\delta^{13}C$ values is not clearly visible. However, we could not exclude that vegetation changes influenced the variability in the $\delta^{13}C$ values of both stalagmites. Furthermore, PCP seems to have a minor influence on the $\delta^{13}C$ values (section 4.2).

4.3.4. Comparison With Meteorological Data

A comparison of the speleothem calcite $\delta^{18}O$ values with mean annual temperature shows a correlation of $r = 0.43$ ($p < 0.001$, $n = 73$) for Zoo-rez-2. Despite a nonsignificant correlation between mean annual

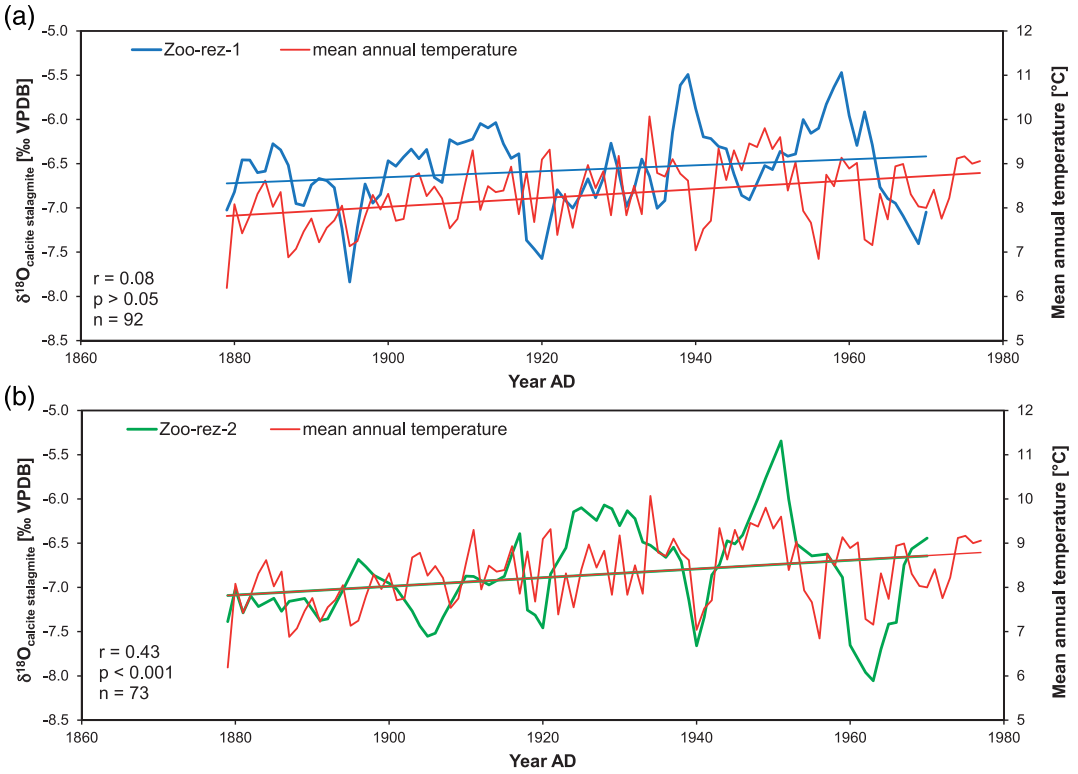

Figure 8. Comparison between mean annual temperature and measured $\delta^{18}O$ values for (a) Zoo-rez-1 and (b) Zoo-rez-2 including long-term trends.

temperature and the $\delta^{18}O$ values of Zoo-rez-1, common patterns are observed between CE 1880 and 1910. The $\delta^{18}O$ values of Zoo-rez-1 and -2 show the same long-term trend as mean annual temperature (Figure 8). This indicates a pronounced influence of mean annual temperature on the $\delta^{18}O$ values of the stalagmites. As discussed above, the mean annual temperature signal could still be preserved in the $\delta^{18}O$ values of the stalagmites in case that the degree of disequilibrium fractionation is constant (Hansen et al., 2019; Mühlinghaus et al., 2009). The other annual proxy records were also tested for correlations with the meteorological data, but no significant correlation coefficients were observed.

4.3.5. $\delta^{18}O$ Values as Proxy for Mean Annual Temperature

The main source for the $\delta^{18}O$ signal in the speleothem calcite is the infiltrating precipitation (Lachniet, 2009), which may be influenced by several processes on the way through the soil and karst as discussed above. On the intraannual scale, mean monthly temperature and mean monthly $\delta^{18}O$ value of precipitation show a high correlation of $r = 0.98$ ($p < 0.001$; $n = 12$; CE 1978–2013; GNIP station Regensburg), which is the expected relation for a midlatitude climate (Rozanski et al., 1993). The relation between temperature and the $\delta^{18}O$ values of precipitation is also significant on the interannual time scale, even if less pronounced with a correlation of $r = 0.63$ ($p < 0.001$; $n = 36$; CE 1978–2013; GNIP station Regensburg). This relation allows us to calculate the $\delta^{18}O$ values of the drip water and speleothem calcite with the model of Wackerbarth et al. (2010). The fractionation factor of Daëron et al. (2019) (equation 7) was used to calculate the $\delta^{18}O$ values of the calcite based on the modeled drip water $\delta^{18}O$ values, as described in section 2.7. The modeled $\delta^{18}O$ values of the speleothem calcite show a correlation of $r = 0.44$ ($p < 0.001$; $n = 36$) with mean annual temperature (CE 1978–2013, meteorological station Bamberg), and this linear regression provides the fundament to extend the model back in time to the time span of CE 1879 to 1970 (meteorological stations Bamberg and Bamberg Observatory). Furthermore, two additional regressions to model the $\delta^{18}O$ values of calcite for the time span of the two speleothems were calculated. For the second one, the mean annual $\delta^{18}O$ values of precipitation were used without any treatment to model the $\delta^{18}O$ values of the drip water. This results in a correlation of $r = 0.63$ ($p < 0.001$, $n = 36$), between modeled $\delta^{18}O$ values

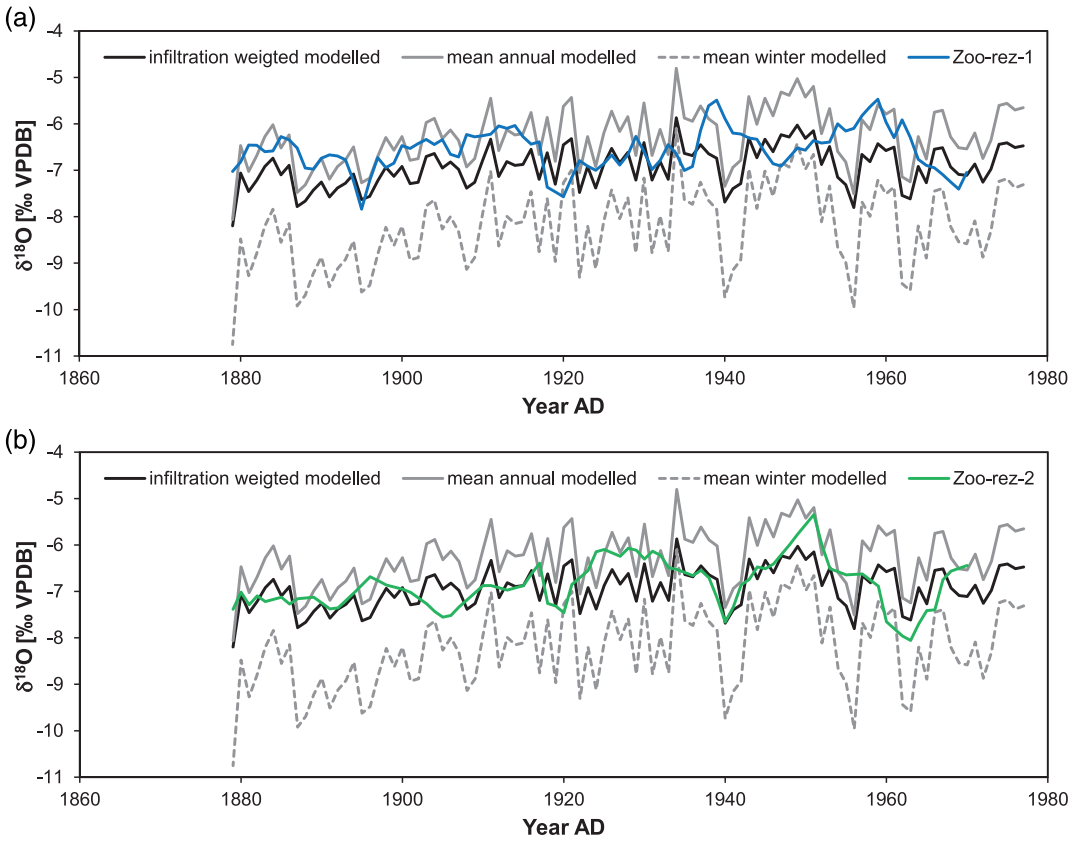

Figure 9. Comparison between the three differently modeled (infiltration-weighted annual mean, annual mean, and annual winter mean) and measured $\delta^{18}O$ values for (a) Zoo-rez-1 and (b) Zoo-rez-2.

and mean annual temperature, which is the same value as for mean annual GNIP $\delta^{18}O$ data correlated with mean annual temperature. For the third regression mean, winter precipitation $\delta^{18}O$ values were used as $\delta^{18}O$ values for drip water, and the resulting correlation of the modeled $\delta^{18}O$ values for calcite with mean annual temperature is $r = 0.67$ ($p < 0.001$, $n = 36$) (detailed description of the calculations, see section 2.7). Comparing the three differently modeled $\delta^{18}O$ series of calcite, the infiltration-weighted

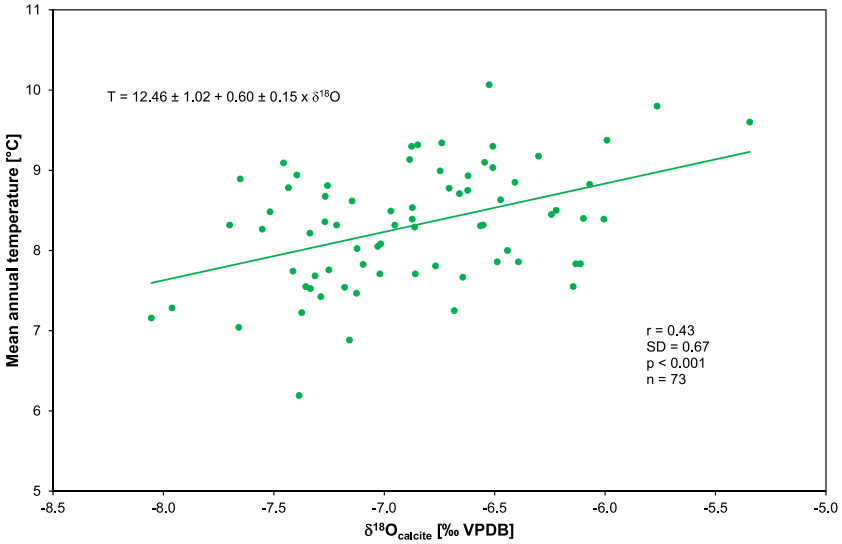

Figure 10. Linear regression between the $\delta^{18}O$ values of Zoo-rez-2 and mean annual temperature.

modeled $\delta^{18}O$ values show amplitudes (2.33‰) and absolute values (mean value -6.93 ± 0.44‰) in the same range as the measured $\delta^{18}O$ values for both stalagmites (mean Zoo-rez-1: -6.57 ± 0.45‰, mean Zoo-rez-2: -6.87 ± 0.53‰) for the time span CE 1879–1970, as well as similar amplitudes (Zoo-rez-1: 2.37‰, Zoo-rez-2: 2.71‰). The model using only the $\delta^{18}O$ values of the winter months shows quite high amplitudes (4.65‰) and distinctly lower values (mean value: -8.22 ± 0.88‰) than the measured values. Even though the 2σ error for this modeled series is 2.02‰, it clearly indicates that infiltration does not only occur during winter months but also—even if to a smaller extent—during summer months as revealed by several cave monitoring studies from the temperate climate zone (Genty et al., 2014; Mischel et al., 2015; Riechelmann et al., 2011, 2017). The model using mean annual $\delta^{18}O$ values shows a bit higher values (mean value: -6.29 ± 0.62‰) than the model using infiltration-weighted $\delta^{18}O$ values. Despite a 2σ error for this modeled series of 1.60‰, it indicates that there is a certain loss of precipitation due to evapotranspiration during the summer months (Figure 9) and that the infiltration-weighted model seems to be most realistic.

Similarly, the slightly increasing trend over time (Figures 8 and 9) is observed in the modeled and the measured $\delta^{18}O$ values. Furthermore, for Zoo-rez-2, the correlation between the measured and the infiltration-weighted, modeled $\delta^{18}O$ values is $r = 0.43$ ($p < 0.001$, $n = 73$). After CE 1935, the correlation between mean annual temperature and measured $\delta^{18}O$ values of Zoo-rez-2 is high, whereas it is low for the older section (Figure 8b). This may be due to missing or false laminae in this section (Riechelmann et al., 2019). The correlation between mean annual temperature and measured $\delta^{18}O$ values of Zoo-rez-1 is insignificant ($r = 0.08$, $p > 0.05$, $n = 92$). However, it is obvious from the time series (Figure 8a) that both show a common pattern before CE 1905. This may also be explained by dating uncertainties due to missing or false laminae, which are estimated to be ± 7 to 19 years in the lower part of the stalagmites, in addition to the dating uncertainty of the top laminae with ± 5 years due to the uncertainty of the detection of the ^{14}C bomb peak (Riechelmann et al., 2019). In addition to these chronological uncertainties, other factors could have an influence on the $\delta^{18}O$ values and result in reduced correlations with mean annual temperature as well as the not existent correlation between the $\delta^{18}O$ values of both stalagmites. These could be changes in the degree of disequilibrium isotope fractionation during precipitation of speleothem calcite, changes in the amount of PCP, or both drip sites could have had different drip rates, as well as differences in the initial drip water chemistry, such as different $SI_{calcite}$ (Riechelmann et al., 2013).

In summary, the overlap with instrumental data provides the opportunity to calibrate measured speleothem $\delta^{18}O$ values with mean annual temperature and provides a fundament for quantitative temperature reconstruction (Figure 10). The resulting regression is given by the following equation:

$$T = 0.60 \pm 0.15 \times \delta^{18}O_{calcite} + 12.46 \pm 1.02. \quad (11)$$

This describes a potential equation to reconstruct quantitative temperatures from the $\delta^{18}O$ values of the calcite further back in time. The standard deviation (SD) for this regression is ± 0.67, which results in a 2σ error of the reconstructed temperatures of ± 1.4°C. This equation can be used for potential speleothem records of the entire Holocene using other stalagmites from Zoolithencave. Nevertheless, these new stalagmites have also to be tested for their response to temperature in the calibration period and by overlapping sections of the stalagmites.

5. Conclusions

The proxy records of the two stalagmites Zoo-rez-1 and -2 are influenced by several factors, which makes their interpretation in terms of past climate variability challenging. Phosphorus and Y, often interpreted as proxies for vegetation and soil activity, are both also influenced by detrital material. Magnesium, Sr, and Ba are affected by weathering of feldspar and clay minerals in the soil and the resulting changes in the silicate to carbonate weathering ratio and to a lesser extent by PCP, as suggested by the positive correlation of Mg and $\delta^{13}C$ values. Weathering of silicates in the soil is increased during warmer and drier conditions, which would also increase PCP and shift Mg, Ba, and Sr in the same direction. Therefore, a distinct interpretation of Mg, Ba, and Sr is not possible.

The $\delta^{18}O$ values of the two speleothems were compared to mean annual temperature, which show a significant correlation of $r = 0.43$ ($p < 0.001$, $n = 73$) for Zoo-rez-2. The $\delta^{18}O$ values of speleothem calcite

were modeled using three approaches of the calculation of the potential $\delta^{18}O$ values of the drip water (infiltration-weighted mean, mean annual precipitation, and mean winter precipitation $\delta^{18}O$ values) and calculating $\delta^{18}O$ values of the calcite under equilibrium isotope fractionation conditions. The regressions between the three differently modeled $\delta^{18}O$ values and the mean annual temperature allow to model the $\delta^{18}O$ values back in time for the timespan of the two stalagmites. The three differently calculated $\delta^{18}O$ series show that the infiltration-weighted modeled $\delta^{18}O$ series correspond best with the measured $\delta^{18}O$ values of both stalagmites. This indicates that infiltration also takes place during the summer months; however, a pronounced portion of the summer precipitation is lost during evapotranspiration. Differences in the older part of Zoo-rez-2 and in the younger part of Zoo-rez-1 between the measured and infiltration-weighted modeled $\delta^{18}O$ data as well as with the mean annual temperature are most probably due to dating uncertainties, resulting from missing and/or false laminae. However, also changes in disequilibrium isotope fractionation, PCP, drip rate, and/or drip water chemistry could result in these differences. The $\delta^{18}O$ values of Zoo-rez-2 show a positive correlation ($r = 0.43$, $p < 0.001$, $n = 73$) with mean annual temperature, which results in a linear regression providing a calibration equation. This would provide the opportunity to calculate quantitative temperatures from stalagmite $\delta^{18}O$ values. Therefore, the speleothem $\delta^{18}O$ values can be used as a proxy for mean annual temperature and provides the basis for the interpretation of older stalagmites from Zoolithencave.

Acknowledgments

D. F. C. Riechelmann, S. Riechelmann, and D. Scholz are grateful to the Deutsche Forschungsgemeinschaft (DFG) (RI 2136/2-1; RI 2136/2-2; RI 2545/3-1; SCHO 1274/9-1; SCHO 1274/11-1), and D. F. C. Riechelmann is grateful to the Johannes Gutenberg University Mainz for funding. We thank the "Forschungsgruppe Höhlen und Karst Franken e.V." for the permission to sample stalagmites from Zoolithencave and the support during the cave trip in CE 1999. For assistance during LA-ICP-MS, we thank B. Stoll and U. Weis from the MPI for Chemistry, Mainz, as well as J. Faust. We thank M. Maus for assistance during stable carbon and oxygen isotope analysis, as well as J. Klose, D. Rupprecht, and M. Veicht for sample preparation of the C/O samples. We thank A. Budsky for help with programming in R. L. Parkner is thanked for assistance with soil sample preparation, T. Reinecke for XRD analyses, as well as K. Krimmler and B. Gehnen for helping with inductively coupled plasma optical emission spectrometer analyses. We thank the Editor B. Williams for his work and two anonymous reviewers as well as S. Carolin for their helpful and constructive comments on the paper. The underlying data are available at NOAA under https://www.ncdc.noaa.gov/paleo/study/28010.

References

Baker, A., Hellstrom, J. C., Kelly, B. F. J., Mariethoz, G., & Trouet, V. (2015). A composite annual-resolution stalagmite record of North Atlantic climate over the last three millennia. *Scientific Reports*, *5*, 10307.

Baker, A., Smart, P. L., Edwards, R. L., & Richards, D. A. (1993). Annual growth banding in a cave stalagmite. *Nature*, *364*(6437), 518–520.

Boch, R., & Spötl, C. (2011). Reconstructing palaeoprecipitation from an active cave flowstone. *Journal of Quaternary Science*, *26*(7), 675–687.

Boch, R., Spötl, C., & Frisia, S. (2011). Origin and palaeoenvironmental significance of lamination in stalagmites from Katerloch Cave, Austria. *Sedimentology*, *58*(2), 508–531.

Borsato, A., Frisia, S., Fairchild, I. J., Somogyi, A., & Susini, J. (2007). Trace element distribution in annual stalagmite laminae mapped by micrometer-resolution X-ray fluorescence: Implications for incorporation of environmentally significant species. *Geochimica et Cosmochimica Acta*, *71*, 1494–1512.

Büntgen, U., Tegel, W., Nicolussi, K., McCormick, M., Frank, D., Trouet, V., et al. (2011). 2500 years of European climate variability and human susceptibility. *Science*, *331*(6017), 578–582. https://doi.org/10.1126/science.1197175

Chan, L.-H., & Hein, J. R. (2007). Lithium contents and isotopic compositions of ferromanganese deposits from the global ocean. *Deep Sea Research Part II: Topical Studies in Oceanography*, *54*(11–13), 1147–1162.

Cheng, H., Edwards, R. L., Shen, C.-C., Polyak, V. J., Asmerom, Y., Woodhead, J., et al. (2013). Improvements in 230Th dating, 230Th and 234U half-life values, and U–Th isotopic measurements by multi-collector inductively coupled plasma mass spectrometry. *Earth and Planetary Science Letters*, *371–372*, 82–91.

Daëron, M., Drysdale, R. N., Peral, M., Huyghe, D., Blamart, D., Coplen, T. B., et al. (2019). Most Earth-surface calcites precipitate out of isotopic equilibrium. *Nature Communications*, *10*(1), 429. https://doi.org/10.1038/s41467-019-08336-5

Deininger, M., Fohlmeister, J., Scholz, D., & Mangini, A. (2012). Isotope disequilibrium effects: The influence of evaporation and ventilation effects on the carbon and oxygen isotope composition of speleothems—A model approach. *Geochimica et Cosmochimica Acta*, *96*, 57–79.

Dettman, D. L., & Lohmann, K. C. (1995). Microsampling carbonates for stable isotope and minor element analysis: Physical separation of samples on a 20 micrometer scale. *Journal of Sedimentary Research*, *65*(3a), 566–569.

Egli, M., Mirabella, A., & Sartori, G. (2008). The role of climate and vegetation in weathering and clay mineral formation in late Quaternary soils of the Swiss and Italian Alps. *Geomorphology*, *102*(3–4), 307–324.

Esper, J., Düthorn, E., Krusic, P. J., Timonen, M., & Büntgen, U. (2014). Northern European summer temperature variations over the Common Era from integrated tree-ring density records. *Journal of Quaternary Science*, *29*(5), 487–494.

Esper, J. F. (1774). Ausführliche Nachricht von neuentdeckten Zoolithen unbekannter vierfüsiger Thiere, und denen sie enthaltenen, so wie verschiedenen andern, denkwürdigen Grüften der Obergebürgischen Lande des Marggrafthums Bayreuth, 148 pp., Nürnberg.

Fairchild, I. J., Borsato, A., Tooth, A. F., Frisia, S., Hawkesworth, C. J., Huang, Y.-M., et al. (2000). Controls on trace element (Sr-Mg) compositions of carbonate cave waters: Implications of speleothem climatic records. *Chemical Geology*, *166*, 255–269.

Fairchild, I. J., & Treble, P. C. (2009). Trace elements in speleothems as recorders of environmental change. *Quaternary Science Reviews*, *28*, 449–468.

Fairchild, I. J., Tuckwell, G. W., Baker, A., & Tooth, A. F. (2006). Modelling of dripwater hydrology and hydrogeochemistry in a weakly karstified aquifer (Bath, UK): Implications for climate change studies. *Journal of Hydrology*, *321*, 213–231.

Fohlmeister, J., Plessen, B., Dudashvili, A. S., Tjallingii, R., Wolff, C., Gafurov, A., & Cheng, H. (2017). Winter precipitation changes during the medieval climate anomaly and the little ice age in arid central Asia. *Quaternary Science Reviews*, *178*, 24–36.

Frisia, S., Borsato, A., Drysdale, R. N., Paul, B., Greig, A., & Cotte, M. (2012). A re-evaluation of the palaeoclimatic significance of phosphorus variability in speleothems revealed by high-resolution synchrotron micro XRF mapping. *Climate of the Past*, *8*(6), 2039–2051.

Fritts, H. C. (1976). *Tree rings and climate*, (p. 567). Caldwell, New Yersey: The Blackburn Press.

Genty, D., Labuhn, I., Hoffmann, G., Danis, P. A., Mestre, O., Bourges, F., et al. (2014). Rainfall and cave water isotopic relationships in two South-France sites. *Geochimica et Cosmochimica Acta*, *131*, 323–343. https://doi.org/10.1016/j.gca.2014.01.043

Groiß, J. T. (1988). *Das Pleistozän in Franken* (pp. 105–115). München: Karst und Höhle.

Häckel, H. (1999). *Meteorologie*, (4th ed.). München: Eugen Ulmer GmbH & Co.
Hammer, O., Harper, D. A. T., & Ryan, P. D. (2001). PAST: Paleontological statistics software package for education and data analysis. *Palaeontologia Electronica*, *4*(1), 9.
Hansen, M., Scholz, D., Schöne, B. R., & Spötl, C. (2019). Simulating speleothem growth in the laboratory: Determination of the stable isotope fractionation (δ13C and δ18O) between H2O, DIC and CaCO3. *Chemical Geology*, *509*, 20–44.
Haude, W. (1954). Zur praktischen Bestimmung der aktuellen und potentiellen evaporation und evapotranspiration. *Mitteilungen des Deutschen Wetterdienst*, *8*(8), 1–15.
Haude, W. (1955). Zur Bestimmung der Verdunstung auf möglichst einfache Weise. *Mitteilungen des Deutschen Wetterdienst*, *11*(2), 1–24.
Heller, F., Niggemeyer, B., Schubert, D., Poll, K., Groiß, J. T., & Huber, F. (1972). *Die Zoolithenhöhle bei Burggaillenreuth/Ofr. 200 Jahre wissenschaftliche Forschung 1771–1971*. Erlangen: Universitätsbund Erlangen-Nürnberg e.V.
Hendy, C. H. (1971). The isotopic geochemistry of speleothems–I. The calculation of the effects of different modes of formation on the isotopic composition of speleothems and their applicability as palaeoclimatic indicators. *Geochimica et Cosmochimica Acta*, *35*, 801–824.
Holz, P., Hartmann, A., Eiche, E., Neumann, T., & Kluge, T. (2018). High-resolution dripwater monitoring—Relationship between modern surface climate signals and cave environment. *Geophysical Research Abstracts*, *20*. EGU2018–18306
Huang, Y. M., Fairchild, I. J., Borsato, A., Frisia, S., Cassidy, N. J., McDermott, F., & Hawkesworth, C. J. (2001). Seasonal variations in Sr, Mg, and P in modern speleothems (Grotta di Ernesto, Italy). *Chemical Geology*, *175*, 429–448.
Jochum, K. P., Scholz, D., Stoll, B., Weis, U., Wilson, S. A., Yang, Q., et al. (2012). Accurate trace element analysis of speleothems and biogenic calcium carbonates by LA-ICP-MS. *Chemical Geology*, *318-319*, 31–44.
Jochum, K. P., Weis, U., Stoll, B., Kuzmin, D., Yang, Q., Raczek, I., et al. (2011). Determination of reference values for NIST SRM 610–617 glasses following ISO guidelines. *Geostandards and Geoanalytical Research*, *35*(4), 397–429. https://doi.org/10.1111/j.1751-908X.2011.00120.x
Johnson, K. R., Hu, C., Belshaw, N. S., & Henderson, G. M. (2006). Seasonal trace-element and stable-isotope variations in a Chinese speleothem: The potential for high-resolution paleomonsoon reconstruction. *Earth and Planetary Science Letters*, *244*(1–2), 394–407.
Kim, S.-T., & O'Neil, J. R. (1997). Equilibrium and non-equilibrium oxygen isotope effects in synthetic carbonates. *Geochimica et Cosmochimica Acta*, *61*(16), 3461–3475.
Kuczumow, A., Genty, D., Chevallier, P., Nowak, J., & Ro, C.-U. (2003). Annual resolution analysis of a SW-France stalagmite by X-ray synchrotron microprobe analysis. *Spectrochimica Acta Part B: Atomic Spectroscopy*, *58*(5), 851–865.
Lachniet, M. S. (2009). Climatic and environmental controls on speleothem oxygen-isotope values. *Quaternary Science Reviews*, *28*, 412–432.
Lang, S. (2000). Höhlen in Franken - Ein Wanderführer in der Unterwelt der Fränkischen Schweiz, 126 pp., Nürnberg.
Maher, K. (2010). The dependence of chemical weathering rates on fluid residence time. *Earth and Planetary Science Letters*, *294*(1–2), 101–110.
Mattey, D., Lowry, D., Duffet, J., Fisher, R., Hodge, E., & Frisia, S. (2008). A 53 year seasonally resolved oxygen and carbon isotope record from a modern Gibraltar speleothem: Reconstructed drip water and relationship to local precipitation. *Earth and Planetary Science Letters*, *269*, 80–95.
Mickler, P. J., Banner, J. L., Stern, L., Asmerom, Y., Edwards, R. L., & Ito, E. (2004). Stable isotope variations in modern tropical speleothems: Evaluating equilibrium vs. kinetic isotope effects. *Geochimica et Cosmochimica Acta*, *68*(21), 4381–4393.
Mischel, S., Scholz, D., & Spötl, C. (2015). $\delta^{18}O$ values of cave drip water: A promising proxy for the reconstruction of the North Atlantic Oscillation? *Climate Dynamics*, *1-16*.
Mischel, S. A., Mertz-Kraus, R., Jochum, K. P., & Scholz, D. (2017). TERMITE: An R script for fast reduction of laser ablation inductively coupled plasma mass spectrometry data and its application to trace element measurements. *Rapid Communications in Mass Spectrometry*, *31*(13), 1079–1087. https://doi.org/10.1002/rcm.7895
Moore, G. W., & Sullivan, G. N. (1978). *Speleology - The study of caves*, (2nd ed. p. 150). Teaneck: Zephyrus Press.
Mühlinghaus, C., Scholz, D., & Mangini, A. (2009). Modelling fractionation of stable isotopes in stalagmites. *Geochimica et Cosmochimica Acta*, *73*, 7275–7289.
Myers, C. G., Oster, J. L., Sharp, W. D., Bennartz, R., Kelley, N. P., Covey, A. K., & Breitenbach, S. F. M. (2015). Northeast Indian stalagmite records Pacific decadal climate change: Implications for moisture transport and drought in India. *Geophysical Research Letters*, *42*, 4124–4132. https://doi.org/10.1002/2015GL063826
Navarra, A., & Simoncini, V. (2010). *A data analysis guide to empirical orthogonal functions for climate*. Dordrecht, Heidelberg, London, New York: Springer.
Okrusch, M., & Matthes, S. (2005). *Mineralogie - Eine Einführung in die spezielle Mineralogie, Petrologie und Lagerstättenkunde*, (p. 526). Berlin, Heidelberg, New York: Springer.
Orland, I. J., Bar-Matthews, M., Ayalon, A., Matthews, A., Kozdon, R., Ushikubo, T., & Valley, J. W. (2012). Seasonal resolution of eastern Mediterranean climate change since 34 ka from a Soreq Cave speleothem. *Geochimica et Cosmochimica Acta*, *89*, 240–255.
Richards, D. A., & Dorale, J. A. (2003). Uranium-series chronology and environmental applications of speleothems. *Reviews in Mineralogy and Geochemistry*, *52*(1), 407–460.
Ridley, H. E., Asmerom, Y., Baldini, J. U. L., Breitenbach, S. F. M., Aquino, V. V., Prufer, K. M., et al. (2015). Aerosol forcing of the position of the intertropical convergence zone since ad 1550. *Nature Geoscience*, *8*(3), 195–200. https://doi.org/10.1038/ngeo2353
Riechelmann, D. F. C., Deininger, M., Scholz, D., Riechelmann, S., Schröder-Ritzrau, A., Spötl, C., et al. (2013). Disequilibrium carbon and oxygen isotope fractionation in recent cave calcite: Comparison of cave precipitates and model data. *Geochimica et Cosmochimica Acta*, *103*, 232–244.
Riechelmann, D. F. C., Fohlmeister, J., Kluge, T., Jochum, K. P., Richter, D. K., Deininger, M., et al. (2019). Evaluating the potential of tree-ring methodology for cross-dating of three annually laminated stalagmites from Zoolithencave (SE Germany). *Quaternary Geochronology*, *52*, 37–50.
Riechelmann, D. F. C., Schröder-Ritzrau, A., Scholz, D., Fohlmeister, J., Spötl, C., Richter, D. K., & Mangini, A. (2011). Monitoring Bunker Cave (NW Germany): A prerequisite to interpret geochemical proxy data of speleothems from this site. *Journal of Hydrology*, *409*(3–4), 682–695.
Riechelmann, S., Schröder-Ritzrau, A., Spötl, C., Riechelmann, D. F. C., Richter, D. K., Mangini, A., et al. (2017). Linking rain, soil, and drip waters at Bunker Cave (W Germany): Insights from long-term monitoring. *Chemical Geology*, *449*, 194–205.
Riechelmann, S., Schröder-Ritzrau, A., Wassenburg, J. A., Schreuer, J., Richter, D. K., Riechelmann, D. F. C., et al. (2014). Physicochemical characteristics of drip waters: Influence on mineralogy and crystal morphology of recent cave carbonate precipitates. *Geochimica et Cosmochimica Acta*, *145*, 13–29.

Rosendahl, W. (2005). Neue Erkenntnisse zur Vorgeschichte der Zoolithenhöhle bei Burggaillenreuth, Nordliche Frankenalb, Süddeutschland. *Die Höhle*, *56*(1–4), 24–28.

Rozanski, K., Araguás-Araguás, L., & Gonfiantini, R. (1993). Isotopic patterns in modern global precipitation. In P. K. Swart, K. C. Lohmann, J. Mckenzie & S. Savin (Eds.), *Climate change in continental isotopic records* (pp. 1-36). Washington, DC: American Geophysical Union.

Rutlidge, H., Baker, A., Marjo, C. E., Andersen, M. S., Graham, P. W., Cuthbert, M. O., et al. (2014). Dripwater organic matter and trace element geochemistry in a semi-arid karst environment: Implications for speleothem paleoclimatology. *Geochimica et Cosmochimica Acta*, *135*, 217–230. https://doi.org/10.1016/j.gca.2014.03.036

Scholz, D., Frisia, S., Borsato, A., Spötl, C., Fohlmeister, J., Mudelsee, M., et al. (2012). Holocene climate variability in north-eastern Italy: Potential influence of the NAO and solar activity recorded by speleothem data. *Climate of the Past*, *8*, 1367–1383.

Scholz, D., & Hoffmann, D. L. (2008). ^{230}Th/U-dating of fossil reef corals and Speleothems. *Quaternary Science Journal (Eiszeitalter und Gegenwart)*, *57*, 52–77.

Scholz, D., Mühlinghaus, C., & Mangini, A. (2009). Modelling δ^{13}C and δ^{18}O in the solution layer on stalagmite surfaces. *Geochimica et Cosmochimica Acta*, *73*, 2592–2602.

Schweingruber, F. H. (1983). Der Jahrring. In *Standort, Methodik, Zeit und Klima in der Dendrochronologie* (pp. 234). Bern: Paul Haupt.

Shopov, Y. Y. (2003). Luminescence of speleothems. *Studi Trentini di Scienze Naturali Acta geologica*, *80*, 95–104.

Sinclair, D. J., Banner, J. L., Taylor, F. W., Partin, J., Jenson, J., Mylroie, J., et al. (2012). Magnesium and strontium systematics in tropical speleothems from the Western Pacific. *Chemical Geology*, *294-295*, 1–17.

Smith, C. L., Fairchild, I. J., Spötl, C., Frisia, S., Borsato, A., Moreton, S. G., & Wynn, P. M. (2009). Chronology building using objective identification of annual signals in trace element profiles of stalagmites. *Quaternary Geochronology*, *4*(1), 11–21.

Tan, M., Liu, T., Hou, J., Qin, X., Zhang, H., & Li, T. (2003). Cyclic rapid warming on centennial-scale revealed by a 2650-year stalagmite record of warm season temperature. *Geophysical Research Letters*, *30*(12), 1617. https://doi.org/10.1029/2003GL017352

R Core Team (2018). R: A language and environment for statistical computing. *R Foundation for Statistical Computing*. Vienna, Austria. Retreived from https://www.R-project.org/

Tipper, E. T., Bickle, M. J., Galy, A., West, A. J., Pomiès, C., & Chapman, H. J. (2006). The short term climatic sensitivity of carbonate and silicate weathering fluxes: Insight from seasonal variations in river chemistry. *Geochimica et Cosmochimica Acta*, *70*(11), 2737–2754.

Tooth, A. F., & Fairchild, I. J. (2003). Soil and karst aquifer hydrological controls on the geochemical evolution of speleothem-forming drip waters, Crag Cave, southwest Ireland. *Journal of Hydrology*, *273*, 51–68.

Treble, P., Shelley, J. M. G., & Chappell, J. (2003). Comparison of high resolution sub-annual records of trace elements in a modern (1911-1992) speleothem with instrumental climate data from southwest Australia. *Earth and Planetary Science Letters*, *216*, 141–153.

Treble, P. C., Chappell, J., & Shelley, J. M. G. (2005). Complex speleothem growth processes revealed by trace element mapping and scanning electron microscopy of annual layers. *Geochimica et Cosmochimica Acta*, *69*(20), 4855–4863.

Tremaine, D. M., Froelich, P. N., & Wang, Y. (2011). Speleothem calcite farmed in situ: Modern calibration of [delta]18O and [delta]13C paleoclimate proxies in a continuously-monitored natural cave system. *Geochimica et Cosmochimica Acta*, *75*(17), 4929–4950.

van Rampelbergh, M., Verheyden, S., Allan, M., Quinif, Y., Chen, H., Edwards, L. R., et al. (2015). A 500-year seasonally resolved δ^{18}O and δ^{13}C, layer thickness and calcite aspect record from a speleothem deposited in the Han-sur Lesse cave, Belgium. *Climate of the Past*, *11*, 789–802.

von Storch, H., & Zwiers, F. W. (2002). *Statistical Analysis in Climate Research* (pp. 293). Cambridge: University Press in Cambridge.

Wackerbarth, A., Scholz, D., Fohlmeister, J., & Mangini, A. (2010). Modelling the δ18O value of cave drip water and speleothem calcite. *Earth and Planetary Science Letters*, *299*(3–4), 387–397.

Warken, S. F., Fohlmeister, J., Schröder-Ritzrau, A., Constantin, S., Spötl, C., Gerdes, A., et al. (2018). Reconstruction of late Holocene autumn/winter precipitation variability in SW Romania from a high-resolution speleothem trace element record. *Earth and Planetary Science Letters*, *499*, 122–133. https://doi.org/10.1016/j.epsl.2018.07.027

Wassenburg, J. A., Immenhauser, A., Richter, D. K., Jochum, K. P., Fietzke, J., Deininger, M., et al. (2012). Climate and cave control on Pleistocene/Holocene calcite-to-aragonite transitions in speleothems from Morocco: Elemental and isotopic evidence. *Geochimica et Cosmochimica Acta*, *92*, 23–47.

Wassenburg, J. A., Riechelmann, S., Schröder-Ritzrau, A., Riechelmann, D. F. C., Richter, D. K., Immenhauser, A., et al. (2020). Calcite mg and Sr partition coefficients in cave environments: Implications for interpreting prior calcite precipitation in speleothems. *Geochimica et Cosmochimica Acta*, *269*, 581–596. https://doi.org/10.1016/j.gca.2019.11.011

Wilson, R. J. S., Luckman, B. H., & Esper, J. (2005). A 500 year dendroclimatic reconstruction of spring–summer precipitation from the lower Bavarian Forest region, Germany. *International Journal of Climatology*, *25*(5), 611–630.

Wimpenny, J., Colla, C. A., Yin, Q.-Z., Rustad, J. R., & Casey, W. H. (2014). Investigating the behaviour of Mg isotopes during the formation of clay minerals. *Geochimica et Cosmochimica Acta*, *128*, 178–194.

Wurth, G. (2002). *Klimagesteuerte Rhythmik in spät- bis postglazialen Stalagmiten des Sauerlandes, der Fränkischen Alb und der Bayerischen Alpen* (PhD thesis, 123 pp). Ruhr-Universität Bochum, Bochum.